

KAUNAS UNIVERSITY OF TECHNOLOGY

DONATAS PELENIS

**RESEARCH OF THE EXCITATION AND RESPONSE SIGNALS
OF CMUT BIOSENSORS**

Summary of Doctoral Dissertation
Technological Sciences, Electrical and Electronic Engineering (T 001)

2020, Kaunas

This doctoral dissertation was prepared at Kaunas University of Technology, Panevėžys Faculty of Technologies and Business, Department of Technologies and Entrepreneurship Competences Centre during the period of 2015–2019.

Scientific Supervisor:

Prof. Dr. Darius VIRŽONIS (Kaunas University of Technology, Technological sciences, Electrical and Electronic Engineering – T 001).

Editor: Prof. Dr. Ramunė Kasperavičienė (KTU)

Dissertation Defence Board of Electrical and Electronic Engineering Science Field:

Prof. Dr. Liudas MAŽEIKA (Kaunas University of Technology, Technological sciences, Electrical and Electronic Engineering, T 001) – **chairman**;

Prof. Dr. Elena JASIŪNIENĖ (Kaunas University of Technology, Technological sciences, Electrical and Electronic Engineering, T 001);

Prof. Dr. Habil Eugenijus KANIUŠAS (Vienna University of Technology, Technological sciences, Electrical and Electronic Engineering, T 001);

Prof. Dr. Habil Arūnas LUKOŠEVIČIUS (Kaunas University of Technology, Technological sciences, Electrical and Electronic Engineering, T 001);

Assoc. Prof. Dr. Ieva PLIKUSIENĖ (Vilnius University, Natural sciences, Chemistry – N 003);

Prof. Dr. Algimantas VALINEVIČIUS (Kaunas University of Technology, Technological sciences, Electrical and Electronic Engineering, T 001).

The official defence of the dissertation will be held at 11 a.m. on 17 April, 2020 at the public meeting of Dissertation Defence Board of Electrical and Electronic Engineering Science Field in Dissertation Defence Hall at Kaunas University of Technology

Address: K. Donelaičio St. 73-403, 44249 Kaunas, Lithuania.

Tel. no. (+370) 37 300 042; fax. (+370) 37 324 144; e-mail doktorantura@ktu.lt.

Summary of doctoral dissertation was sent on 17th March, 2020.

The doctoral dissertation is available on the internet <http://ktu.edu> and at the library of Kaunas University of Technology (K. Donelaičio St. 20, 44239 Kaunas, Lithuania).

KAUNO TECHNOLOGIJOS UNIVERSITETAS

DONATAS PELENIS

**CMUT BIOJUTIKLIŲ MIKROSTRUKTŪRŲ ŽADINIMO IR
ATSAKO SIGNALŲ TYRIMAS**

Daktaro disertacijos santrauka
Technologijos mokslai, elektros ir elektronikos inžinerija (T 001)

2020, Kaunas

Disertacija rengta 2015-2019 metais Kauno technologijos universiteto Panevėžio technologijų ir verslo fakulteto Technologijų ir verslumo kompetencijų centre.

Mokslinis vadovas:

Prof. dr. Darius VIRŽONIS (Kauno technologijos universitetas, technologijos mokslai, elektros ir elektronikos inžinierius – T 001).

Redagavo: Prof. dr. Ramunė Kasperavičienė (KTU)

Elektros ir elektronikos inžinerijos mokslo krypties disertacijos gynimo taryba:

Prof. dr. Liudas MAŽEIKA (Kauno technologijos universitetas, technologijos mokslai, elektros ir elektronikos inžinerija - T 001) - **pirmininkas**;

Prof. dr. Elena JASIŪNIENĖ (Kauno technologijos universitetas, technologijos mokslai, elektros ir elektronikos inžinerija - T 001);

Prof. habil. dr. Eugenijus KANIUŠAS (Vienos technologijos universitetas, technologijos mokslai, elektros ir elektronikos inžinerija - T 001);

Prof. habil. dr. Arūnas LUKOŠEVIČIUS (Kauno technologijos universitetas, technologijos mokslai, elektros ir elektronikos inžinerija - T 001);

Doc. dr. Ieva PLIKUSIENĖ (Vilniaus universitetas, gamtos mokslai, chemija – N 003);

Prof. dr. Algimantas VALINEVIČIUS (Kauno technologijos universitetas, technologijos mokslai, elektros ir elektronikos inžinerija - T 001).

Disertacija bus ginama viešame Elektros ir elektronikos inžinerijos mokslo krypties disertacijos gynimo tarybos posėdyje 2020 m. balandžio 17 d. 11 val. Kauno technologijos universiteto disertacijų gynimo salėje.

Adresas: K. Donelaičio g. 73-403, 44249 Kaunas, Lietuva.

Tel. (370) 37 300 042; faks. (370) 37 324 144; el. paštas doktorantura@ktu.lt.

Disertacijos santrauka išsiųsta 2020 m. kovo 17 d.

Su disertacija galima susipažinti internetinėje svetainėje <http://ktu.edu> ir Kauno technologijos universiteto bibliotekoje (K. Donelaičio g. 20, 44239 Kaunas).

INTRODUCTION

Biosensors are currently on the agenda of medical equipment developers. Scientists and technology companies devote considerable effort and resources to designing and developing low-cost informative biosensors. More and more spheres of application of such sensors emerge ranging from specific biomolecule detection technologies to automated therapy [1]. Some biosensor systems are based on the use of microelectromechanical structures (MEMS) [2-6]. In 2015, R. Fogel conducted an extensive overview of acoustic wave-operated biosensors existing in the market, showing that microprocessor-based technology is capable of providing a much higher quality of biosensor signal processing [7]. Computing technology that is becoming faster and cheaper enables the hardware part of biomedical devices to be reduced, thus reducing their cost, especially in mass production cases. In addition, the unmatched flexibility of software solutions offers even more applications for biosensors [8].

Among the specific, technical and technological challenges that developers of biosensors face are functional sensor verification and calibration. To solve these issues, extensive experimental research is being carried out and various signal processing methods devoted to the processing of biosensor received signals are being applied, issues of noise to signal ratio are being solved as well [2]. However, it is obvious that methods of verification and calibration that are widely used in other measurement technology branches are not sufficient for biosensors. Because the use of biosensors only makes sense in a wildlife environment, the verification and calibration technique cannot be transposed linearly from areas specific to other sensor types. For example, in many cases, the operation of biosensors is based on a long incubation period during which biological interactions occur between the object being analyzed and the functional part of the sensor. Over a long period of time, not only can indefinite and uncontrolled influence of the environment on the results occur, but the biological object itself may change: denature, grow, change its location, etc. [4].

One of the most widely known and most promising types of biosensors is based on the measurement of analyte mass and other physical properties, using specific biochemical interactions and gravimetric principles [9]. The use of MEMS, and in particular microfluidic chip-integrated microcavity and capacitive micromachined ultrasonic transducer (CMUT) technologies, provides reasonably good competition for optical, photonic, biochemical and other methods [2]. Although the use of microcantilever in molecular mass spectrometry has been acknowledged, the CMUT structure, which has been demonstrated in real-time bio-interaction measurement in liquid media, has a much greater potential for practical applications [3, 10]. Previous studies have shown that CMUT-based sensors are capable of detecting and measuring the interaction of biomolecules with the environment, such as the evaluation of bovine serum albumin (BSA)

protein in a liquid medium in the measurement of acoustic wave propagation time [9]. Previous work has also shown that the specific biochemical interaction between an antibody and an antigen may be determined by gravimetric measurement when the CMUT structure operates in a gaseous environment under resonant mode [12–15]. However, the latter method is unsuitable for real-time applications, since the resonant frequency of the CMUT structure in a liquid where biochemical interaction between the antibody and the antigen normally occurs cannot be informative. E. Sapeliauskas and others [16] have proposed to use a secondary interdigital-like CMUT structure and transverse Scholte-type waves for the detection of biochemical interactions in a liquid. However, the conventional signal processing algorithms used in their work are non-adaptive and unsuitable unless the operating conditions of the sensor are carefully controlled. This prevents the proposed technology from being used in mass products. To process the signal, innovative techniques based on artificial neural networks, which have excellent adaptability and can efficiently process non-linearly changing biosensor received signals, may be employed [10-13].

Besides the problems of signal processing, there are also issues of control, mixing of microfluids, which are operated by biosensors, and bio-object positioning. Various biochemical tests include mixing of two fluids, for example, during DNA purification, polymerase chain reaction (PCR), immune complex formation, enzyme and protein coupling. The results of such processes, tests or measurements depend on the quality and rapid mixing of samples and reagents. In microfluidic systems, the Reynolds number denoting the relationship between inertia and viscosity forces is usually lower than 100 [14-16]. This means that, during the measurement of the biological interaction under the laminar liquid stream, the studied bio-elements move through the microchannel without mixing, which results in a reduction of the biological interaction speed and, thus, the useful signal size [17, 18]. In the case of the introduction of analytical fluids into the microchannel, if no forced mixing is applied, the kinetic change of the fluids takes from 30 seconds to 2 minutes, depending on the microchannel dimensions and fluid flow.

The growing interest in microchannel systems has stimulated recent research, focusing the microchannel-integrated CMUT biosensor on the microscopic analysis systems (μ TAS) market, where a single biochemical/electromechanical system can address multiple challenges: measurement, fluid pumping, mixing, and biological element positioning. Considerable attention is being paid to the adaptation of microelectromechanical system technologies in complex liquid microsystems so that devices may function not only as received signal estimators but also as liquid control systems [9, 19-21]. The integration of MEMS structures into biosensors can be beneficial not only because they may be smaller in size than analogous liquid micropumps and mixers, but also because of the integration of this technology into various

previously developed biosensor systems. Previous work has shown that CMUT biosensor technology may be more sensitive due to the low mass of resonant structure membranes and has a higher energy transfer efficiency than analogous piezoelectric transducers with similar functions. Biosensors using the CMUT structure can operate in a wide variety of acoustic modes, which is not typical for most MEMS devices based on the piezoelectric effect. For example, the fundamental CMUT structure may be much easier to use for phased transmitting or receiving transverse or surface acoustic waves because it has a natural ability to divide the surface of the device into many independently exciting elements. Previous studies have shown how directional acoustic pumping and fluid mixing in a CMUT-type biosensor microchannel may be performed using a two-phase secondary structure [8, 22, 23].

Relevance of work

Biosensors are currently widely used in various research fields. In medicine, they are used to detect tumors, pathogens, high blood glucose levels and toxins. For the past few decades, scientists and researchers have been working on the development of various biosensor technologies [2, 8] that enable diagnosis, evaluation and monitoring of processes with biological elements, ensuring qualitative and quantitative parameters. Currently, biosensor systems are classified by application and detection spheres. Depending on the employed principle of transduction, they are divided into electrochemical, mass and optical [24-27]. Biosensor systems can also act as classifiers capable of assessing changes in the interaction of proteins, nucleic acids, enzymes, saccharide oligonucleotides, and ligands. Based on the types of the analyte, biosensor systems may be modified to detect DNA, glucose, toxins, microtoxins, drugs or enzymes. In biological detection, quantitative parameters of interaction with biological elements, such as antibody binding to antigen, are most often monitored [6, 28, 29].

Previous research studies have shown that capacitive micromachined ultrasound transducers (CMUTs) may be used to detect biological elements. CMUTs differ in their production, operation and application from MEMS biosensors based on piezoelectric materials. Each developed biosensor technology requires solving issues related to both technological design and service processes as well as methods of biochemical interaction analysis. CMUT-based biosensors are no exception. This thesis uses a transverse acoustic wave biosensor radiating at the interface of a liquid and a solid body, such a biosensor is adapted to work in a fluid medium and may function as a device for biological interaction detection and monitoring, as well as for microstream control and biologically active element positioning. Previously developed versions of biosensors [2] have a number of technical drawbacks associated with various types of instrumental and natural noise. Natural sources of noise include the specific effects of substances of biological origin: protein degeneration, denaturation, and other biochemical effects that are constantly present in bioactive systems. These effects cannot be

stabilized by technical means and, therefore, require specific signal processing techniques with high resistance to uninformative interference. The excited acoustic wave in the biosensor propagates through all elements of the sensor structure: silicon, liquid, or microchannel walls. Meanwhile, useful information is carried by the transverse Scholte-type wave propagation time and its energy changes. Therefore, biosensors need the flexibility and adaptability of signal processing algorithms to eliminate uninformative interference. To evaluate biosensor readings under such conditions, multiparametric algorithms that measure changes in the information wave caused by biological interactions work best. Due to its energy conversion efficiency, CMUT technology is suitable not only as an environmental or interaction estimator but also as an execution device meant for the precise positioning of bioactive elements in the microchannel [17, 30-32].

The aim of the thesis is to design a transverse wave delay measurement technique using sensors with a CMUT interdigital-type structure and the method with increased resistance to various noise sources.

Research problem

Previous studies have shown that mechanical, dynamic measurement of the properties of biological elements by MEMS devices is useful for quantitative and qualitative diagnostics of bioelements. On the other hand, whatever the high sensitivity potential of the resonant CMUT transducer, the resonant mode is not suitable for real-time biosensors due to the high suppression in liquid operation. Because the CMUT-type biosensor consists of two CMUT transmitter and receiver interdigital-like structures, and an area for the analyte in the middle, the biochemical interaction may be detected by measuring acoustic wave delay. However, the current signal processing methods are not always suitable for processing signals received with such a CMUT structure. The information comes from more than one simultaneous channel and the signal to noise ratio is low. Due to the noise in the signal and the complexity of the received signal, there are limitations on the signal processing speed and the sensitivity. Therefore, there is a need for a signal processing and interpreting methodology improving the signal to noise ratio, which would be suitable for economically feasible technical realization. The problem formulated in this work is addressed by creating and analysing an innovative method of signal processing based on the use of a convolutional artificial neural network capable of operating with microcontrollers, microcomputers, or programmable logic arrays.

Research hypothesis

Specific signal processing algorithms with high flexibility and adaptability may significantly improve the useful signal to noise ratio of biosensors operating by the principle of Scholte wave delay measurement. Biosensor electromechanical structures, normally used for wave delay measurement, may be employed for

pumping and mixing of analytical liquids, as well as positioning of biologically active particles in a one or two axis system, alternating with the sensor function.

Objectives

1. To investigate currently employed methods of transverse acoustic wave delay measurement and their applicability to a CMUT-based biosensor.
2. To create and analyse the neural network-based acoustic wave delay measurement algorithm, applicable to a CMUT biosensor and compare quantitatively with other known algorithms and measurement techniques.
3. To use the created algorithm in experiments monitoring the deposition of biologically active elements in the analyte zone of the biosensor and to describe them.
4. To examine the possibilities of using the electromechanical CMUT structure of the biosensor for microfluid pumping, mixing and positioning of biologically active particles.
5. To characterize microfluidic pumping from the energy point of view.
6. To investigate the possibilities of using CMUT sensor microstructures for positioning biologically active particles in one and two-axis coordinate systems.
7. To evaluate the thermal loss of the biosensor in harmonic mode.

Scientific value

The developed biosensor signal processing methods and digital as well as analytical models will result in the more accurate interpretation of biochemical interactions ongoing in a CMUT-based biosensor microchannel, by flexibly adapting to changing measurement medium and microchannel parameters.

The artificial neural network-based signal processing algorithm demonstrated in the thesis will allow creating a signal processing system with exceptional resistance to noise and change of measurement conditions.

The created method for modelling acoustic flow in a microchannel will allow modelling acoustic waves excited by phased CMUT finger groups. This method is based on the methodology of biological elements, fluid manipulation and deposition in the CMUT biosensor microchannel.

The practical value of research results

The knowledge gained during the work will allow simplifying the calibration of CMUT-type biosensors working in the microfluidic environment and obtaining a better signal to noise ratio, thus reducing the dependence on the measurement medium and other measurement conditions. The developed methods of signal processing and acoustic wave modelling will be used to design prototype biosensor structures and electronics ensuring their operation.

Hypotheses

Application of artificial neural networks to CMUT biosensor signal processing may result in signal-to-noise ratio improvements of up to 15 dB.

A biochemical interaction may be detected by interpreting the delay kinetics of transverse waves propagating between liquid and solid.

The interdigital-type CMUT biosensor may also be used as an execution device to control the position of biologically active particles in a one- or two-axis system.

Thesis approval

The main results of the doctoral thesis have been published as 5 articles in the journals listed in International Scientific Indexing (ISI) list of journals with an impact factor and as 2 presentations at international scientific conferences.

Thesis structure and volume

The thesis consists of an introduction, four chapters, conclusions, a list of references and a list of author's publications. The total volume of the thesis is 99 pages, 44 figures, 3 tables and 125 bibliographic references.

1. SURFACE ACOUSTIC WAVE BIOSENSORS AND SIGNAL PROCESSING METHODS

1.1. Surface acoustic wave biosensors

1.1.1. CMUT-based interdigital type finger biosensors

Capacitive micromachined ultrasonic transducers were first used as biosensors in 2008. Khuri-Yakob and colleagues suggested applying the CMUT type resonating transducer in detection of biological element mass deposited on CMUT membranes. This biochemical detection transducer is classified as the resonating chemical sensor [33]. Upon modification of CMUT cell membranes with polymer material, the resonant sensor was successfully adapted to operate as a chemical transducer for detection of gas concentrations [34]. The first CMUT resonance-based immuno-sensor was demonstrated by Ramanavičius, Viržonis and colleagues in 2013 [9].

The first CMUT interdigital type sensors were proposed by McLean in 2002 [35, 36]. The structure was implemented with 2 parallel interdigital fingers separated by a distance of a quarter wavelength. A CMUT interdigital finger structure may expediently generate wave energy by simultaneously changing the interdigital finger phase shift. Mechanical energy generated according to the given method propagates in the solid-liquid interface. Such a structure is adapted to detect liquid analyte according to the integrated resonant frequency of the received acoustic wave. As recently as 2014, Viržonis and colleagues adapted the sensor according to the integrated biosensor received resonant frequency to detect a biological interface and determine liquid concentrations [3, 37, 38].

1.2. Application of surface acoustic wave biosensors

A biosensor consists of 2 components: a system for biochemical interface detection and a transducer that converts the biochemical (biological) response to

a measurable output electric signal [25]. For the SAW device to be used as a biosensor, it has to be coated with a biospecific layer corresponding the analyte. Immobilising chemicals depend on the surface of a SAW device, which may be selective. Functionalised thiols may be used on gold surfaces, while silicon or SiO₂ surfaces may be used with different silanes. Both methods are employed for attachment analysis of active monolayer specific molecules or, if needed, for combination of the major intermediate layers, for example, hydrogels. A SAW biosensor surface modifier does not depend on the detection method [21]. The main SAW type sensor configuration is presented in Fig. 1. A SAW biosensor is composed of finger pairs, which may operate like a mechanical or electric energy generation device. Surface mounted interdigital pairs are attached to signal generation and reading equipment.

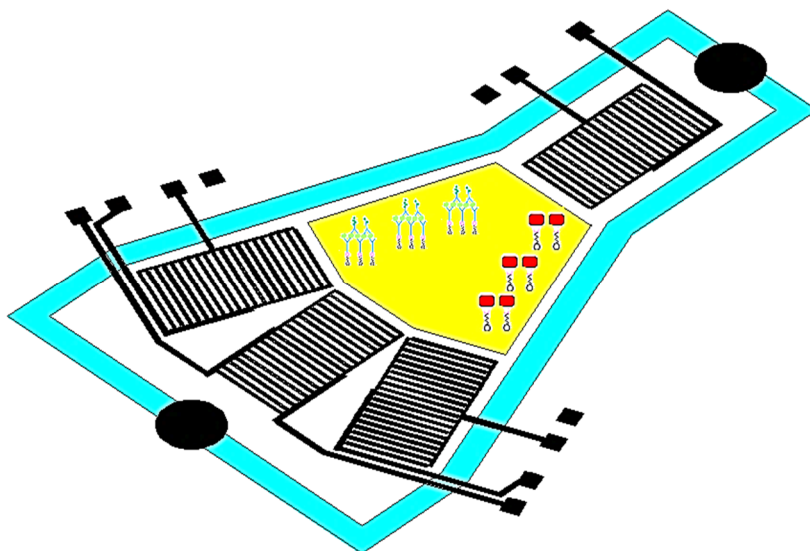


Fig. 1. A biosensor using the interdigital type structure with an area in the middle for detection of a biological interface

There is an analyte area between the interdigital groups. Specific molecules (e.g., antibodies) are immobilized on the biosensor area meant for the analyte so that later biological elements (e.g., antigens) would attach to specific molecules. On the selective analyte area, specific molecules attached to an antigen affect the characteristics of the propagating acoustic wave [39-41].

1.3. Processing methods of biosensor response signals

Measuring signal delay time is one of the main methods used in this thesis. Delay time may also be referred to as signal propagation time, signal arrival time,

delay duration. This method is widely used in ultrasound measurements, such as non-destructive control, ultrasound imaging and diagnostic devices, sonars. In biosensors with transverse surface acoustic waves, methods of measuring wave propagation time (signal delay) are applicable when the interaction of biological elements with the analytical part of the biosensor changes the speed of acoustic wave propagation [14, 42].

The traditional, most common signal delay time measurement is the measurement of the time elapsed between the initiation of the excitation pulse and the moment of detection of the signal passing through the analytical area of the biosensor (hereinafter – biosensor response or biosensor received signal). This method is further referred to as single-pulse delay measurement in this thesis. The potential single-pulse delay measurement accuracy increases with decreasing duration of the excitation signal, so that the CMUT structure on the transmitter side is excited by a signal of 1–3 harmonic periods. The received signal of the biosensor in the receiver part is converted into an electrical signal with the detection moment registered according to the local maximum of an oscillation amplitude [43]. To calibrate the delay signal measurement channel, a reference phantom with the known delay time or calculated with the needed precision may be employed.

In the thesis, the biosensor received signal is processed in 7 different methods:

1. Single-pulse delay measurement method;
2. Delay determination by cross-correlation;
3. Delay determination by signal interpolation;
4. Delay determination by signal approximation with an empirical curve;
5. Delay determination by envelopes;
6. The signal smoothing method;
7. Received signal processing by a convolutional artificial neural network.

The results of signal processing in quantitative units are presented in chapter

1.4. Liquid streaming in a microchannel medium

The traditional liquid stream generation devices are implemented via the piezo element substrate, on which interdigital type fingers connected to an impulse generator are mounted. Via the connected CMUT fingers, the generator distorts the surface, thus creating transverse acoustic waves [14-16, 42]. When generated waves propagate within a liquid and solid structure, the greater part of energy is propagated at the Rayleigh angle θ_R to the liquid.

$$\theta_R = \arcsin\left(\frac{v_f}{v_r}\right); \quad (1)$$

where v_r – acoustic wave velocity on the surface of the solid structure, m/s; v_f – acoustic wave velocity in the fluid, m/s.

The Rayleigh angle of refractive energy to the fluid depends on the velocity ratio. The result of the liquid streaming effect also depends on the geometric dimension of a microchannel and the type of microchannel material, which may result in a destructive effect, not allowing the liquid stream to form. To compensate this, the interdigital type architecture applied in CMUT type biosensors may be used. CMUT interdigital type finger pairs in a biosensor are composed of two finger groups separated by a distance of $\lambda/4$ [35, 36, 43]. This structural advantage allows controlling the propagating energy angle regardless of the fluid type present in the microchannel and geometric as well as substance variables of the microchannel.

2. RESEARCH METHODOLOGY

2.1. Design of CMUT interdigital type biosensors

The arrangement of CMUT cells in a biosensor is illustrated in Fig. 2. The black outline consists of CMUT cell arrays, which are arranged as interdigital fingers. Symbol p defines the spacing between the fingers that are connected to one common electric array. Parameter W refers to the width of the interdigital type structure. Unlike in piezoelectric solutions where the interdigital type pair composes only one finger, CMUT cell-based fingers are composed of the lower and the upper electrodes, between which there is a vacuum gap. One of the major CMUT advantages is the fact that twice as many fingers, composed of CMUT cells, are possible in the same area, which allows to direct acoustic wave energy to a specific direction.

In this thesis, double iteration transducers are used. In some transducers, CMUT cells are designed to operate at a 10 MHz resonant frequency in the fluid, while in others they are designed to operate at a 5 MHz frequency in the fluid. The spaces in interdigital type finger arrangement depend on the CMUT cell resonant frequency: they have to coincide with the propagating acoustic wavelength. In the other case, it will be impossible to process the interdigital finger-generated and received waves due to a weak signal.



Fig. 2. CMUT biosensor layout

On a scaffold of designed biosensors (silicon) operating at a 5 MHz resonant frequency, four interdigital groups of 20 fingers each are designed. The spacing between the fingers $p = 300 \mu\text{m}$ reflects the transverse acoustic wavelength, which propagates at a 1,480 m/s velocity within the liquid-solid interface. The biosensor consists of two groups of transmitter and receiver finger pairs, which are composed of 2 interdigital type fingers, separated by a space $p_1 = \lambda/4$. This arrangement technology allows controlling the direction of the transverse acoustic wave. Between the transmitter and receiver fingers, there is an area designed for a 100-nm gold thickness biological interface (analyte). The distance between the transmitter and the receiver is $L_I=14.7 \text{ mm}$ and the length of the analyte area is $G_p=10 \text{ mm}$. By analogy, transducers operating at a 10 MHz resonant frequency in the liquid were designed. The distance between the fingers is $p = 146 \mu\text{m}$ and the distance between the interdigital finger groups, the transmitter and the receiver is $L_I=11 \text{ mm}$, $G_p=8 \text{ mm}$. Such a type of structure is composed of 20 pairs as well. The production and assembling procedures of transducers are described in the next section.

2.2. CMUT biosensor manufacture, characterization and assembling

The CMUT biosensors used in the experiments were produced by two different assembling technologies. The first described technology is based on the sacrificial release methods, which were used to manufacture transducers operating at a 10 MHz resonant frequency in the liquid. Biological element kinetics and liquid stream experiments in this work were performed with these biosensors. Lower frequency biosensors (5 MHz) were produced based on the wafer bonding technology. The transducers were used for experiments of measuring and processing the received acoustic wave signal.

In this study, microchannels of two different materials and two structures were used. Some microchannels were made from polydimethylsiloxane and some from acrylic glass. The microchannel made from acrylic glass (see Fig. 3a) was processed with a programmable milling machine. The 0.3-mm² tubes with liquid analyte connections were horizontally added into the microchannel, which was mounted together with the biosensor through the 100- μm thick polyamide tape with a cut microchannel 3 mm in width and 12 mm in length.

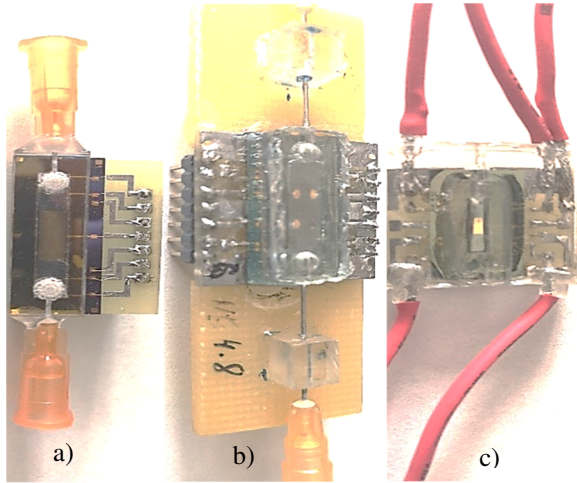


Fig. 3. In experiments, CMUT biosensors with different types of channels were used. a) – a 5 MHz biosensor with a closed organic glass microchannel; b) – a 10 MHz closed biosensor with a PDMS microchannel; c) – a 10 MHz open biosensor with a PDMS channel

Open (see Fig. 3c) and closed (see Fig. 3b) type microchannels were made from polydimethylsiloxane (PDMS). In a PDMS closed channel, liquid connections to the external liquid pumping device were designed.

2.3. Assessment of acoustic wave propagation delay

Measurement of acoustic wave propagation delay may be performed by various signal processing methods, such as cross-correlation, envelope, etc. In this thesis, traditional methods of acoustic wave propagation delay assessment are compared with an innovative artificial neural network-based algorithm. In order to describe the results obtained using the method proposed in this thesis, the comparison is performed with traditional signal processing methods.

The experiment was conducted with a biosensor operating at a 5 MHz resonant frequency in the liquid. It's interdigital fingers were arranged at distances of 300 μm . For readings of the received acoustic wave, we used FLUKE 196C two-channel oscilloscope, connected to a low-noise amplifier. The experiment was conducted with isopropyl alcohol, and a solution of isopropyl alcohol and deionized water (at a ratio of 1:200). The acoustic wave propagation delay was measured by one or the other signal processing method (see Fig. 4).

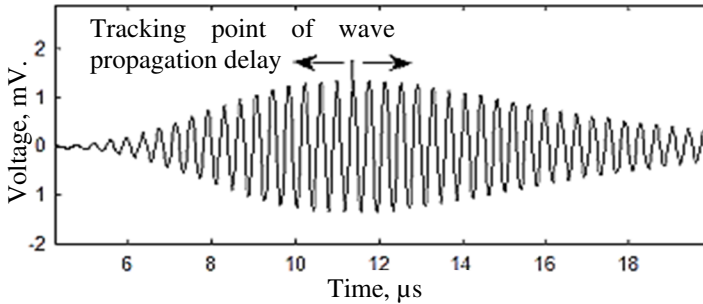


Fig. 4. Assessment of wave propagation delay by monitoring the change in one peak or one peak group in time

During the experiment, acoustic wave time and voltage data were recorded and stored as primary unprocessed material, which was used as a database for signal propagation delay processing by analytic methods. Experiment results and signal processing are described in the results section.

2.4. Processing of CMUT biosensor acoustic wave signals by artificial neural networks

This section presents a methodology for biosensor signal processing used for signals of biosensors with a delay line, by using various methods of signal approximation, correlation and interpolation. The results of such signal processing are compared with the new proposed signal processing methodology where neural networks with convolutional primary processing are applied. The conducted study demonstrates a significant signal to noise ratio increase when a trained convolutional artificial neural network is applied for analysis of wave propagation measurement results. The experiments were conducted using CMUT interdigital type biosensors.

The implementation of the method is complex and consists of a few stages. First, the demonstration of acoustic wave propagation delay processing methods using correlation, envelope, interpolation and combined time signal processing methods was performed. Other sections present methods like convolutional type networks, applied for classification of biosensor readings according to acoustic wave propagation delay. A convolutional artificial neural network is trained to operate as a biosensor received signal spectrogram, which demonstrates acoustic wave signal power according to the time-frequency domain. Spectrograms are composed of FDTD modelling results and experimental data. The real biosensor geometric dimension is applied to define the model in a FDTD environment. Model environment parameters (density, velocity, attenuation) are selected using the delay correlations with a mean square deviation algorithm. Model parameters are correlated on the basis of experimental results, obtained on isopropyl alcohol.

2.5. Use of convolutional neural network for processing of biosensor response signal

The experiment preparation stage is illustrated in Fig. 5. The microchannel is connected with a biosensor device through a 100 μm polyamide tape with a cut 20 \times 3 mm aperture. The tape connects a biosensor silicon structure with a microchannel making a hole which is 100 μm in height and 3 mm in width, filled with the analysed liquid. Two 0.3-mm liquid connections are added into the microchannel for pumping the analysed liquid via an external peristaltic pump. In the experiment, one of the CMUT interdigital structures is connected to the signal generator (3, Agilent 33522A), and control contacts on the other side of the interdigital type structure are connected via a transmit/receive switch (6, TX810) to a low-noise amplifier (LNA-AD8432). The amplified signal is connected to an oscilloscope (8, FLUKE 196C). The CMUT structures of the assembled biosensor are supplied with a 30V direct voltage (5, Agilent N7752). The wave propagation velocity is influenced by temperature: therefore, the results are compensated taking into account the temperature of the liquid pumped in and out. To measure the temperature, digital thermocouples are used.

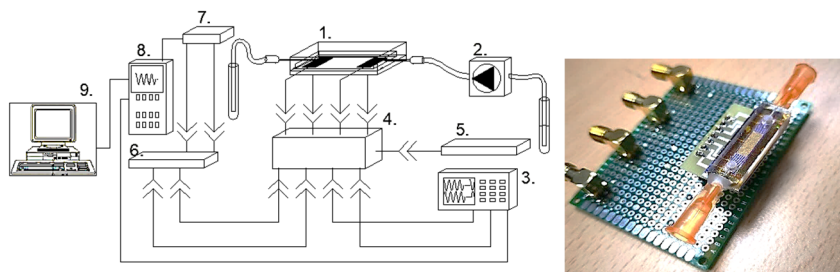


Fig. 5. Biosensor maintenance equipment used in experiments: 1 – biosensor; 2 – peristaltic pump; 3 – signal generator; 4 – BIAS; 5 – direct voltage source; 6 – transmitter/receiver signal switch; 7 – low-noise amplifier; 8 – two-channel oscilloscope; 9 – computer; on the right, a fully assembled biosensor with a microchannel

The aim of the first experiment was to verify the trained CNN. In the experiment, standard reference liquids were used: deionized water, isopropyl alcohol and 0.9% physiological solution. The liquids were used in the experiment with known parameters like density and acoustic wave propagation velocity. In the experiment, the biosensor microchannel was filled with a standard reference liquid and the measurement system was turned on. The recorded signal is transformed into a spectrogram and presented to a trained network in an expectation that the trained convolutional neural network will determine the received signal wave propagation delay, which will allow measuring wave propagation velocity between the liquid and solid structure.

In the second experiment, two different signal processing methods were compared: the trained convolutional network and the methodology for wave propagation delay measurement by envelope tracking when its received signal is processed with a band pass filter. The results are described in the results section. Bovine serum albumin (BSA) was used in the experiment to determine the deposition dynamics of biological material on the golden area of the biosensor analyte at different BSA concentrations (0.1 mg/mL; 1 mg/mL; 3mg/mL). Determination of BSA deposition dynamics has been performed in many biochemical experiments and in our previous works when a biosensor resonant frequency change, rather than wave propagation delay, was used to determine concentration. BSA deposited on gold attaches by forming a monolayer of biological elements, which changes the properties of acoustic wave propagation in the liquid-solid interface, which in turn affects wave propagation delay.

2.6. Liquid stream control in a microchannel by a CMUT interdigital type finger structure

Resonant frequency of capacitive micromachined ultrasonic transducers depends on mechanical transducer load. Other important parameters are geometric dimensions: the distance between the transmitter and the receiver as well as between CMUT cell fingers. Control parameters are selected depending on the finger arrangement geometry. These parameters are used to create in a microchannel a directionally operating force which enables liquid pumping and mixing. Via finger groups, the energy generated to the liquid creates the Gor'kov potential. Depending on reflections formed in a microchannel, which are affected by liquid medium and microchannel geometric parameters, nodes are formed in the fluid where force-caused pressure occurs. The Gor'kov potential defines the position of manipulated particles in a microchannel.

The geometric environment of the liquid stream dynamics medium is defined according to the architecture of CMUT transducers operating at a 10 MHz resonant frequency, used in the experiments (presented in section 2.1). In the first stages of modelling, force parameters are selected to create force and radiation directions in a microchannel (see Fig. 6).

The transducer is composed of interdigital pairs separated by a space of $\lambda/4$. By changing the excitation stage of these fingers, the direction energy of generation is changed, on the influence of which a fluid stream is formed in the microchannel. In the first stage of modelling, it is demonstrated how CMUT type transducers may create the Rayleigh refractive wave effect. This effect is defined as the force vector, calculated according to the wave propagation velocity within the liquid and the transverse wave velocity of the solid structure. In the second stage of modelling, based on the refractive wave effect and more than one interdigital finger group, the Gor'kov potential is applied in biological element positioning. The method is grounded on two separate interdigital type finger

arrays, the forces of which sum up thus creating constructive and destructive interference. The force potential is presented as pressure. In locations with the lowest pressure, manipulated particles are accumulated (see Fig. 7).

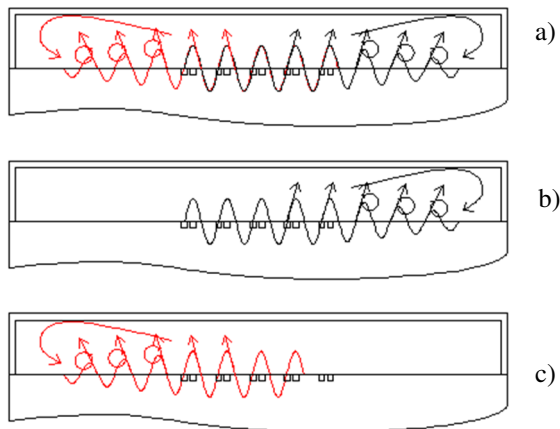


Fig. 6. Control of acoustic stream direction, by changing the excitation stages of transducer fingers: a) 0° phase shift; b) -90° phase shift; c) $+90^\circ$ phase shift

Fig. 7 shows the control methodology where the Gor'kov potential is generated in a microchannel by application of CMUT finger pair groups. The result might be applied in positioning microspheres or biological elements. In order to justify this method, dynamic modelling was performed, which showed that the FDTD method reveals through the effect of finger group interface that may be used to control the liquid stream and microspheres or biological elements in a microchannel.

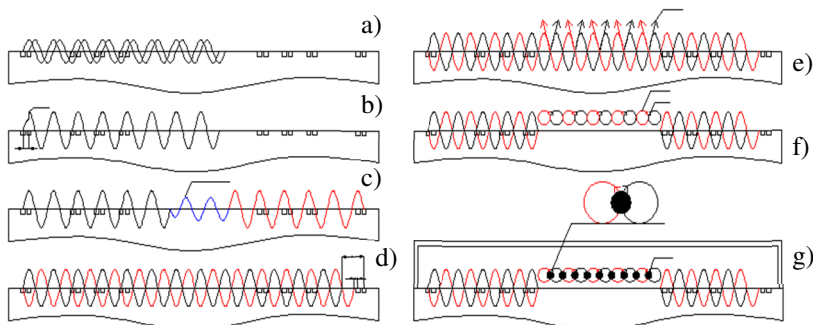


Fig. 7. Stages of microsphere and biological element positioning: a) establishing 2 interdigital type finger (transmitter) pairs to generate transverse acoustic waves; b)

balancing finger excitation by regulating signal generator phases; c) enabling receiver fingers to generate transverse acoustic waves (a–b stages); d) balancing transmitter and receiver fingers so that transmitter- and receiver-generated transverse acoustic waves overlap at 180° ; e) the transducer immersed into a liquid medium radiates acoustic energy at the Rayleigh angle to the liquid; f) radiated acoustic energy to the liquid creates a rotational energy transfer effect, which repeats itself at a wave propagation length; g) radiating transmitter and receiver refractive waves at the Rayleigh angle produces $\lambda/2$ rotational forces in the opposite directions, which further generate the lowest acoustic pressure. After adding microspheres, smaller than a wavelength, into the liquid, they are positioned into the lowest pressure area.

In order to justify the model, experiments with 15- μm size polyester fluorescent microsphere mixed with deionised water at a proportion of 0.003 $\mu\text{g}/\text{mL}$ were conducted. The microspheres were infiltrated into the microchannel. CMUT interdigital type transducers separated by a space of $\lambda/4$ were excited with a standing acoustic wave. By changing the transducer interdigital pair shift phase, we assessed the radiation caused by acoustic waves in liquid mixing, pumping and microsphere positioning. The experiment was recorded on a 0.8 MP camera with a 10x zoom function.

2.7. Diffusion kinetics and acoustic flow measurement

The experimental structural scheme of a liquid diffusion and acoustic stream measurement system is presented in Fig. 8. Liquid stream in the biosensor was maintained by using a peristaltic pump, which was connected to the biosensor microchannel by 0.5 mm silicon tubes.

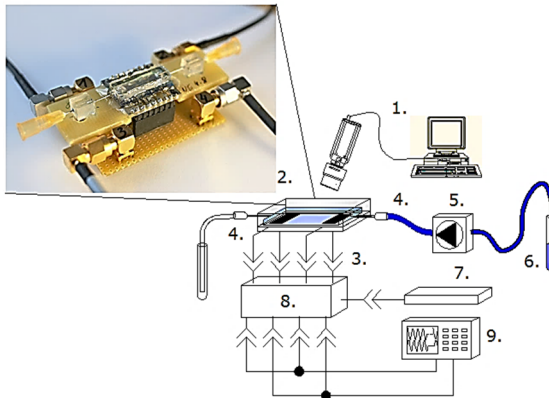


Fig. 8. Diffusion kinetics and liquid acoustic pumping measurement scheme: 1 – a camera; 2 – a microchannel with integrated interdigital type fingers; 3 – electrical connection contacts of a transducer; 4 – liquid connection contacts; 5 – a peristaltic pump; 6 – colour/transparent liquid storage; 7 – direct voltage source; 8 – BIAS; 9 – signal generator

For control, electric contacts of the biosensor are connected to a direct voltage source and signal generator. To measure the acoustic streaming, the microchannel system was filled with a coloured liquid or microspheres. Liquid diffusion kinetics in a microchannel was recorded on a video camera.

To process the image, a software algorithm was developed and the visual material was analysed according to the speed of colour change or microspheres. The video was segmented into shots. In the first stage of algorithm implementation, the mask filter was applied and uninformative areas in the visual material were eliminated. From the informative area matrix, the average value was calculated and represented on a time scale according to the shot time. Thus, the streaming kinetics in a biosensor may be assessed. By measuring the speed of movement of the microspheres, the microspheres are identified in each frame and the displacement is calculated by comparing their position in the two adjacent camera frames. From the displacement and knowing the time difference between adjacent frames and the velocity of the microspheres is calculated.

2.8. Biochemical interaction measurement and kinetics

Experiments conducted with biologically active materials allowed us to assess the sensitivity range of biosensor kinetic interface. Bovine serum albumin (BSA) concentrations with a 0.9% physiological solution were used in the experiment. Concentrations of 0.1 mg/mL, 1 mg/mL and 3 mg/mL were used. When BSA solutions are added into a microchannel, depending on the concentration size and duration, the biosensor analyte area adsorbs BSA elements, resulting in change of electric measurement units of a biosensor received signal, for example, CMUT integrated resonant frequency or wave propagation delay. In order to assess the influence of acoustic streaming on the biological interface, we conducted a study to determine the dependence of BSA component kinetics on the BSA concentration size. In the second stage of the experiment, the BSA element deposition experiment was conducted where transverse acoustic waves were applied. New sensors were used in each stage of the experiment.

3. RESEARCH RESULTS

3.1. Verification results of biosensor received signal

To characterize the experimental data by estimating the acoustic waves generated on the biosensor, the transmitter interdigital-type fingers are excited by a single high-frequency pulse, both in the FDTD model and in the actual experiment. Verification of the model involves experimental measurements of the received signal with liquid samples of known characteristics, such as deionised water with an acoustic wave speed of 1,481 m/s (20°C) and a density of 997 kg/m³. The model describes a transducer base with a longitudinal acoustic wave velocity in silicon of 8,433 m/s, a transverse acoustic wave velocity of 5,840 m/s, and a density of 2,329 kg/m³. The upper part of the biosensor has a microchannel with

longitudinal acoustic wave velocity of 1,713 m/s in acrylic glass, transverse acoustic wave velocity of 1,189 m/s, and density of 1,181 kg/m³.

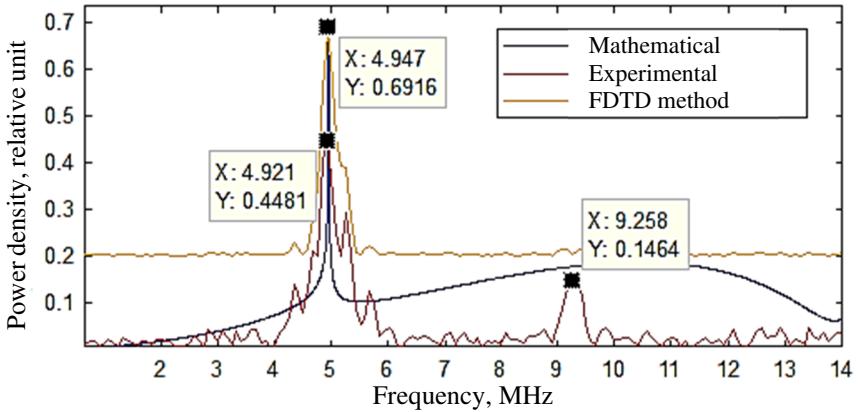


Fig. 9. CMUT-based biosensor received signal verification through the frequency domain

In the course of the experiment, a time domain signal is read from the biosensor and converted to frequency response. Within the signal, the maximum frequency characteristic peaks are identified and the finite-time difference model is matched. The search for the physical parameters of the environment is automated by applying an identifying algorithm for finding the frequency change of the frequency domain.

The analytical method provides the phase acoustic wave velocities, which are converted into the frequency domain according to the geometric dimensions of the applied transducer interdigital fingers. The received signal frequency band in the analytical method is calculated according to the periodic spacing of the CMUT finger positions ($\lambda - 300 \mu\text{m}$).

Frequency is calculated by dividing the phase velocity of the analytical model by the finger placement period. Discussion of the results in the graph (Fig. 9) shows the predominance of peaks at 5 MHz. This peak describes the transverse acoustic wave propagation between a liquid and a solid substance. Comparison of the results of experiments and FDTD with the analytical model shows that the informative signal which can describe the biochemical interaction is only at 5 MHz. Other formed peaks describe other phase velocities obtained from reflections or other modes in the biosensor layers.

3.2. Determination of acoustic wave propagation delay by mathematical methods

For experimental measurements, a concentration of isopropyl alcohol with deionised water (1:200) was used. The experiment was performed with a 5 MHz

resonant frequency biosensor (in water) with the interdigital fingers spaced 300 μm . To obtain the experiment adequacy, it was repeated 5 times. The FLUKE 196C dual-channel oscilloscope was used to receive the acoustic wave. During the experiment, the peristaltic pump was used to fill the microchannel with 0.4 mL/min of isopropyl alcohol. After 50 seconds, the liquid was changed from isopropyl alcohol to a solution of isopropyl alcohol in deionised water. After 550 seconds, the peristaltic pump inlet was returned to isopropyl alcohol. The results of the experiment are presented in Fig. 10, which shows the findings in 5 methods determining the acoustic wave propagation delay.

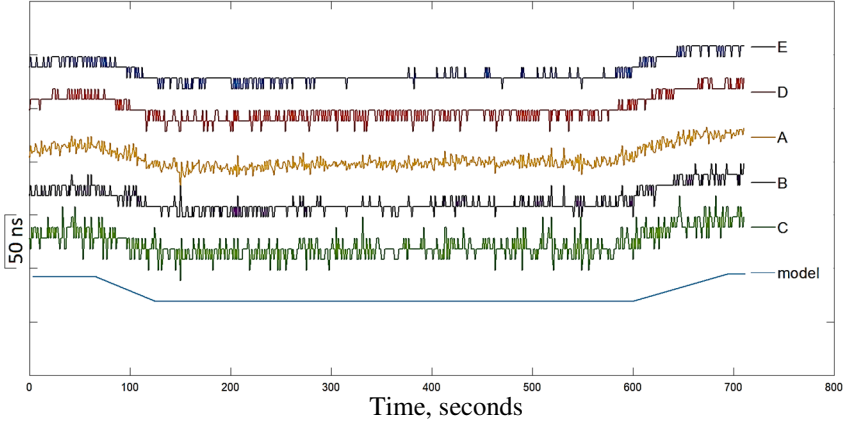


Fig. 10. Signal processing methods comparison. Illustrating strips show for 30 ns reference of signal change experiments.

The results show the estimated received signal wave propagation delay, which was processed by 5 different signal processing methods. Some signal processing methods were combined because of noise in the measurement system that distort the results.

In the first case, when attempting to estimate the biosensor wave propagation delay, the envelope method failed due to the high frequency and low frequency noise generated in the signal. Intermediate signal processing, a band pass filter, was required to estimate the wave propagation delay. The most popular method used to determine the acoustic wave propagation delay is the phase shift measurement method. In this case, the noise figure calculation method was used to compare the signal processing methods. The calculation methodology is given in expression (3).

$$N_f = 10 \lg \left(\frac{|S_m|^2}{\left| \frac{1}{k} \sum_{n=1}^k |M - S_m|^2 \right|} \right); \quad (2)$$

where S_m – modelled signal, M – average of measured signal noise RMS [44].

Table 1. Comparison of signal processing methods by the signal noise ratio

A, dB	B, dB	C, dB	D, dB	E, dB
64,89	63,46	58,87	59,90	65,56

To summarise the comparison, we can see that the maximum signal to noise ratio of 65.65 dB is obtained in the E case when an adaptive bandpass filter and delay measurement are performed by cross-correlation. The lowest ratio is obtained in the case of C (58.87 dB) when using the envelope maximum method without any further signal processing. The latter method of measurement delay was used in our previous work [45, 46]. A noticeable improvement in the signal to noise ratio may also be obtained by interpolation algorithms and high-resolution time axis synthesis. Thus, the signal to noise ratio improvement of up to 6.67 dB may be achieved by employing the most appropriate signal processing technique and appropriate delay measurement method.

3.3. Application of the convolutional network for identification of liquid media

Fig. 11 shows a CNN signal processing fragment. The image on the left shows the signal received during the experiment. The center image shows the spectrogram converted from the received signal, and the image on the right shows the error map of the trained convolutional network. The classifier error map represents the estimated noise in the received signal, which shows that elimination of the noise may be inefficient even in the narrow bandwidth filter. In the error map (Fig. 11), yellow colour is used to represent the informative part of the signal activated by the convolution operation and filtered using the ReLu function. The transition from blue to yellow means that the fragments are identical in terms of different fluid characteristics of the analysed signals.

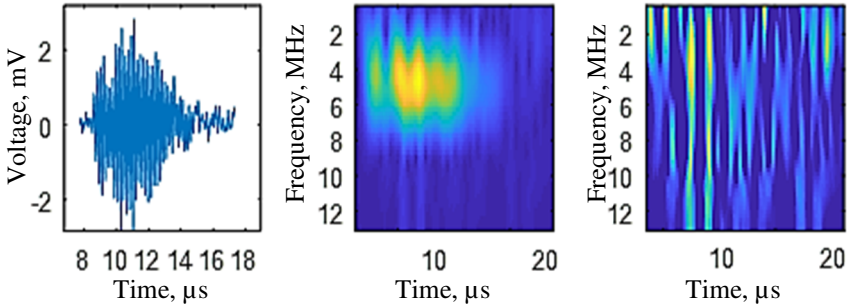


Fig. 11. Measured signal processing with the trained CNN network. The figure on the left shows the measured signal in the time and voltage scale. The figure in the center

shows the measured signal spectrogram, introduced to the trained CNN network. The figure on the right side shows the signal mismatch map (activation).

The results of the experiment verifying the trained convolutional network are shown Table 2. The table provides statistics describing the percentage of undetected real and modelled signals. The lowest error rate was estimated by network verification with isopropyl alcohol.

Table 2. Application of trained CNN in detection of the liquid

Substance	Wave propagation velocity in the liquid, m/s	Density, kg/m ³	Modelled signal mismatch (%)	Measured signal mismatch (%)
Deionised (20°C)	1,481	997	1.5	9.1
Isopropyl alcohol (20°C)	1,170	786	1.1	6.6
Physiological solution 0.9% (20°C)	1,450	1,040	1.8	11.4

Finite time difference model was based on experimental results performed with isopropyl alcohol. This was influenced by the inferior adhesion interaction in water and physiological solution, which has been previously observed and described by our group colleagues[32, 47].

The better the adhesion of the liquid in the solid-liquid interface, the greater the amplitude of the measured acoustic wave. Dozens of duplicate experiments were performed to validate the results. Known parameter fluids were used to validate the trained convolutional network. The highest error detection rate was verified in a physiological solution, reaching up to 11.4%. Such results were obtained due to poor watering of the silicon surface, which is higher compared with the modelled signal amplitude. A greater amount of unrecognised findings was influenced by the fact that during the experiment the liquids were changed. In a microchannel when liquids are changed, their concentrations change, which further affects both the wave propagation velocity and the density of the liquids.

3.4. Assessment of convolutional neural network sensitivity

Real-time experiments were performed with the aim to find a practical advantage of the convolutional trained network application method for biosensor signal processing. Section 3.2 compares signal processing methods for the biosensor signal analysis, used in previous work, with a CNN classifier algorithm trained on the basis of the results of a finite-time difference method. The finite-time difference modelling results were additionally supplemented with various levels of electrical signal noise. Fig. 12 demonstrates the results of comparison between the two different signal processing methods. In the experiment, liquids of

different mechanical properties that have influence on the biosensor received propagation delay are changed. The middle line of the figure shows the results of the signal generated by the FDTD method, which are compared with the signals above and below. The upper curve of the figure shows a wave propagation delay in the case of the trained CNN network. The curve in the lowest position illustrates the analytical (band pass filter with an envelope maximum tracking algorithm) result of the received signal processing. At the beginning of the experiment, deionized water is added at $0.4 \text{ cm}^3/\text{min}$ debit through the biosensor microchannel.

The compared results of the signal processing methods with those of the FDTD method show greater fluctuations of higher frequencies in each processed curve. These fluctuations may be explained as noise that occurs due to the measuring devices. In processing a signal with a band pass filter with an envelope tracking method algorithm, the measurement results are limited by a sampling rate of 9 ns. To obtain results with a higher signal sampling rate, a larger sampling rate measuring device is required.

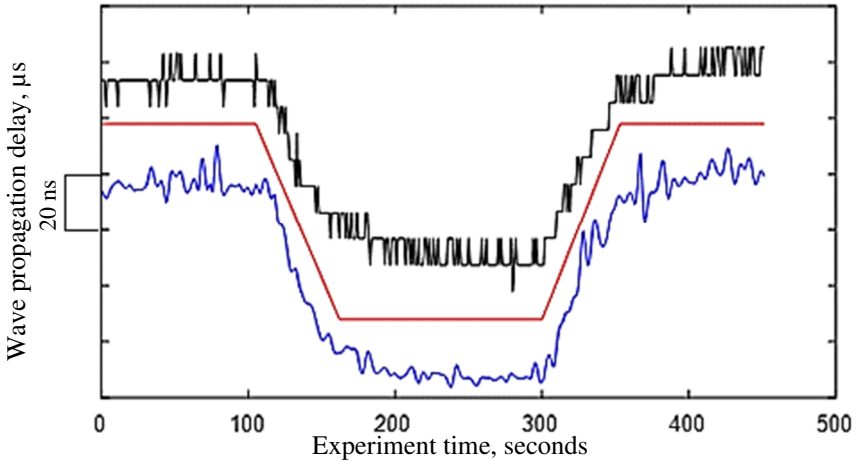


Fig. 12. Measurement of wave propagation delay in the real time. The liquid change stages in the experiment are as follows: deionised water > physiological solution 0.9% > deionised water. The signal wave propagation delay was calculated from a 20 μs received signal. Assessment of wave propagation delay using a band pass filter is shown at the top, while using the trained convolutional network – at the bottom.

On the contrary, the CNN processing methods has no signal quantisation effect, resulting in a more even distribution of the fluctuation amplitude. By eliminating dynamic fluid diffusion effects in the signals and applying noise window estimation methods, the signal-to-noise ratio is assessed. The signal-to-noise ratio using a band pass filter is 60 dB. Meanwhile, it is 75 dB when a trained

CNN network is used. The signal-to-noise ratio improves by 15 dB when using CNN for signal processing.

In the next signal processing method, the sensitivity experiment was performed with bovine serum albumin (BSA), which was deposited on the biosensor analyte (gold) area. Previous studies have defined that a monolayer is formed upon proteins binding on the gold surface. Thus, the BSA material is suitable for verification of the biosensor function. Fig. 13 shows the results of the experiment with different water and BSA solutions. By means of solutions, BSA is deposited on the analyte area of the biosensor. Before the experiment, 4 concentrations of BSA and water solution were prepared, mixing deionised water and BSA concentrate. During the experiment, the received signal was processed with a trained CNN classifier and smoothed to eliminate the noise generated by the used devices (instrumental noise).

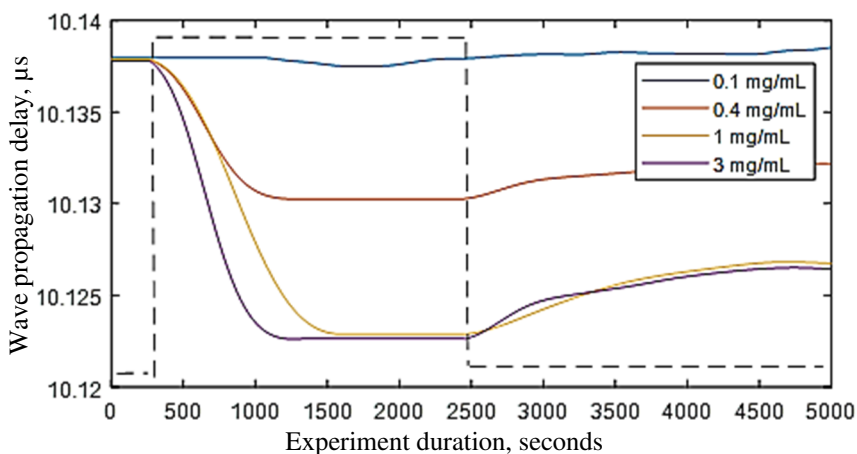


Fig. 13. BSA protein deposition on the biosensor selective area. The dotted line: high level means BSA and water concentration; low level means water.

The analysis of Fig. 13 shows that curves of different levels and dynamics form with different BSA amounts in the water. As BSA settles on the biosensor, the propagation delay of the acoustic wave changes. Almost all concentrations of BSA solutions show an effect on the measured signal, except at 0.1 mg/mL BSA. After BSA has been deposited, deionised water is again added into the microchannel, after which the wave propagation delay stabilises to its initial value. The change in wave propagation delay is related to the change in density of the materials being measured. As the density of BSA is greater than that of water, the wave propagation delay in the signal is reduced. The wave propagation delay does not return to its initial value after water is added (from 2,500 seconds), due to the formation of a BSA protein monolayer on the selective biosensor area. The higher

dynamics between 1 mg/mL and 3 mg/mL concentrations can be explained by the emergence of higher density in the microchannel. However, after the channel flush procedure, at either 1 mg/mL or 3 mg/mL, the signal stabilises to similar levels of wave propagation delay. It can be assumed that the entire analyte site is covered with BSA protein. In the experiment with BSA concentration of 0.1 mg/mL, no radical change between solution and water was observed. It may be argued that the resolution of the measurement device and the digitization period are too small to capture the interpretable change in wave propagation delay.

3.5. Acoustic liquid streaming control

The CMUT interdigital type fingers generate a mechanical wave propagating from solid-liquid interface that transfers part of the energy to the liquid microchannel medium at each wave period due to ultrasound diffraction. This effect is non-linear due to the attenuation and viscosity parameters. When the acoustic wave is attenuated as it is transmitted to the liquid medium, due to the relationship between the inertia and the viscosity forces with the geometry of the channel and the liquid parameters, dynamic liquid streaming effects appear. Depending on the environment and the layout of ultrasonic transducers, fluid mixing, pumping and manipulation effects can be created in the microchannel.

To evaluate the effect of liquid pumping, a long-term microchannel was additionally modelled, in which the generated directional force creates a fluid pumping effect (Fig. 14).

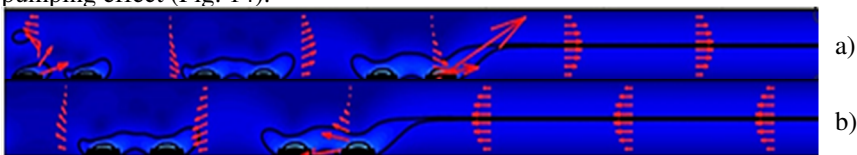


Fig. 14. The liquid pumping dynamics model in a microchannel when CMUT finger pairs are excited with a continuous sinusoidal shape at different excitement phase shifts: a) -90° ; b) $+90^\circ$

The model shows that the highest pumping effect of the liquid is in the middle of the microchannel. At the sides, the liquid stream is lower due to viscosity forces. Fig. 14 shows how force created with the same CMUT fingers acts on the liquid in the direction of force generation. When experiments on liquid colour change diffusion and experiments measuring biological elements were conducted, a fully enclosed microchannel with laterally introduced fluid inlets was used. An external peristaltic pump was used in the experiments, which created an additional flow of the fluid in the microchannel. This principle is shown in the model results (see Fig. 15).

The arrows on the left side of the model represent the input of the fluid stream into the microchannel, while on the right side there is an output of the fluid stream from the microchannel. The flow rate of the inlet liquid into the

microchannel is the same. By exciting the CMUT fingers, force is created that acts in the direction of external flow (b) and against the direction of external flow (a). By the generated CMUT finger force, which acts in the direction of flow movement, the fluid in the microchannel flows along the bottom of the microchannel. If the force generated by the fingers acts against the flow, the fluid in the microchannel flows on the surface of the microchannel. Applying this effect to real-world conditions allows acoustic power to control biochemical and mixing interactions in fluids.

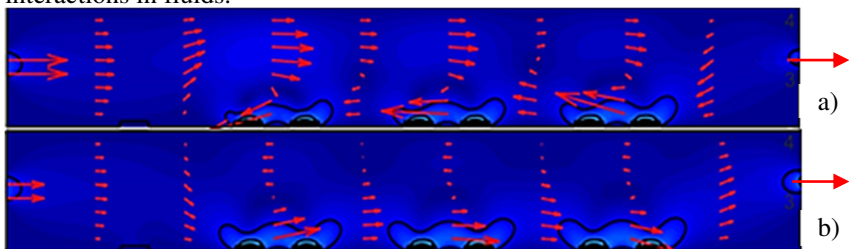


Fig. 15. The liquid dynamics model in a microchannel with an external liquid stream inlet and outlet when CMUT finger pairs are excited with a continuous sinusoidal shape at different excitement phase shifts: a) -90° ; b) $+90^\circ$

To control the liquid flow, an experiment was performed, which was aimed at determining the fluid pumping rate. The experiment was performed using 10 MHz interdigital-type biosensors with an interdigital spacing of $148 \mu\text{m}$. The transducer was equipped with a $100\text{-}\mu\text{m}$ high organic glass microchannel with liquid debit connections. In the experiment, the microchannel was filled with $15 \mu\text{m}$ fluorescent polystyrene microspheres (density $1,055 \text{ kg/m}^3$) and deionised water (density $\sim 1,055 \text{ kg/m}^3$) at a ratio of 1:10.

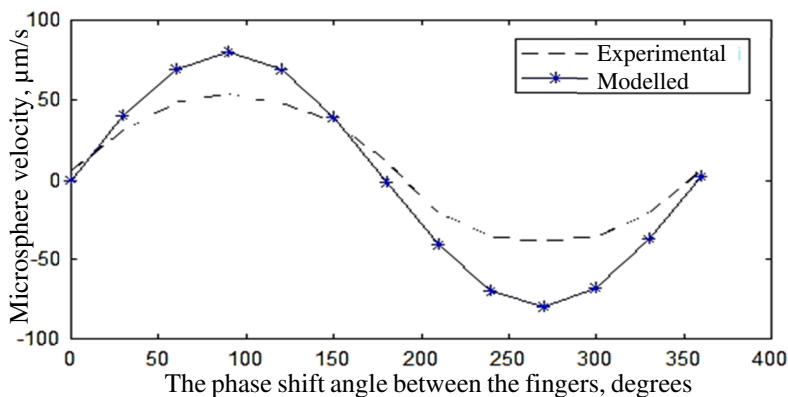


Fig. 16. Liquid pumping results

In the experiment, the phase shift of biosensor interdigital finger pairs was changed. The video camera was used to assess the microsphere movement velocity in the microchannel. During the experiment, the phase shift of the sinusoidal excitation signal between the CMUT interdigital fingers was altered (see Fig. 16). The obtained results were compared with the model results. Excitation of transducer pair fingers through a 0° or 180° phase shift resulted in equal propagation of transducer-generated energy power direction on both sides. The comparison of experimental and modelled results showed a difference in the total phase shift. The results were affected by the transducer total inclination angle. The greatest microsphere movement velocity was recorded when transducer finger pairs were excited at 90° and 270° (-90°) phase difference. The direction of microsphere movement was different. Assessment of the liquid pumping efficiency according to the microchannel geometric dimension and microsphere movement velocity demonstrated that the liquid-affecting power was 4 pW, while total CMUT transducer power was 16.4 mW.

3.6. Acoustic streaming kinetics

In the experiment with coloured and painted liquids, liquid diffusion was observed in the biosensor microchannel. The liquid was pushed through the microchannel by a peristaltic pump at a $0.1 \text{ cm}^3/\text{min}$ debit. In the first stage, the microchannel was filled with a transparent liquid, when the microchannel was filled, experiment recording was started using the video camera. After 10 seconds, the peristaltic pump was stopped and the transparent liquid was changed to the coloured liquid. The results were processed following the methodology described above. We assessed the acoustic power and pumping velocity ratio and performed several repeated experiments keeping the transverse acoustic wave direction the same in all the experiment. To validate the results, dozens of repeated experiments were conducted. The results of the experiments are presented in the graph (Fig. 17).

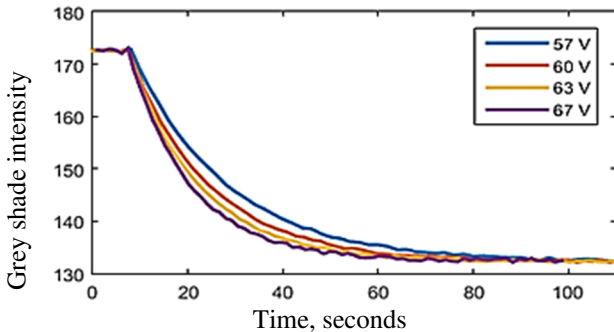


Fig. 17. The increased direct (BIAS) voltage of CMUT transducers increases the liquid mixing effect.

During the experiment, the biosensor CMUT cell voltage was changed within 57–67 V range. The result shows that increasing CMUT cell power increases the intensity of liquid mixing because of increased acoustic energy.

3.7. Group interdigital finger interface in the control of liquid streaming

The chapter “Liquid stream control in a microchannel by a CMUT interdigital type finger structure” described the effect of CMUT interdigital type finger-generated force to the liquid, when liquids are pumped and mixed. This summary of the study results shows how acoustic power generated by CMUT interdigital finger groups affects the liquid in the microchannel. The expression of acoustic wave velocity modelling is integrated into the liquid dynamics model through the Gor’kov expression. This method is aimed at creating acoustic “tweezers”, which may block the biological element position by pressure nodes in the microchannel. By simultaneously changing the CMUT finger group phases, the position of acoustic tweezers in a microchannel may be changed. Fig. 20 demonstrates the marginal modelling results when the phase difference of CMUT two finger group was altered. The force radiating to the microchannel was calculated according to the maximum value of the total force generated by the fingers of each group, while generating the force towards the middle of the microchannel horizontal.

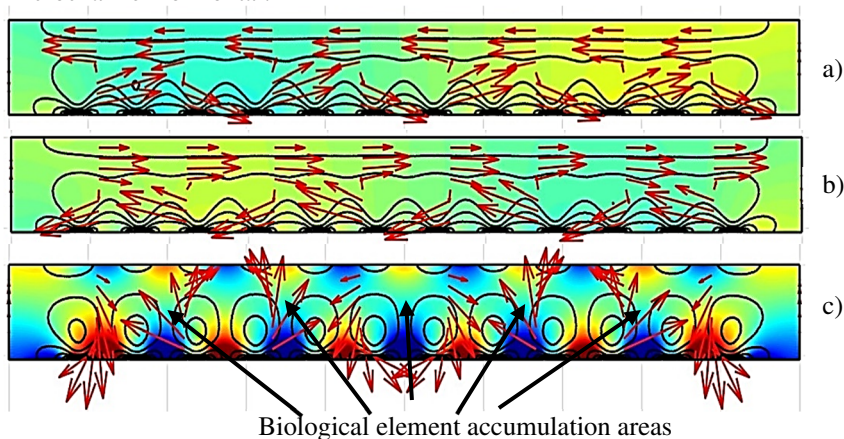


Fig. 18. Pressure finger formation in the microchannel through control of CMUT finger groups. The figure demonstrates the total force of two finger groups when the phases between the finger groups pass by at: a) 20°; b) 90°; c) 180°.

Fig. 18 shows the pressure distribution in the microchannel: cold colour (blue) marks the negative direction pressure, and warm colour (red) marks the positive direction pressure. The arrows indicate the direction in which the liquid is affected by the energy of the CMUT interdigital groups. Black oval shapes

outline how the liquid moves. The illustration shows that the liquid in the microchannel rotates in a circle. The finger groups of the CMUT transducers generate energy along the horizontal axis to the inner side of the microchannel, with the phases extending less than or more than 180° , creating a liquid pumping effect in the microchannel. The force exerted on the two sides of the liquid is balanced when the finger groups of the CMUT are excited by a 180° shift. The force ratio is then the same at each wavelength, forcing the liquid to move in a rotational contour every $\lambda/2$. In other cases, the vector of the total energy force generated by the interdigital groups directs the liquid to move in a certain direction. The Gor'kov output describes the location where the positioning elements will accumulate in the microchannel. Accumulation of biological elements occurs at the lowest pressure values when the pressure is closest to zero (Fig. 18c Biological element accumulation areas).

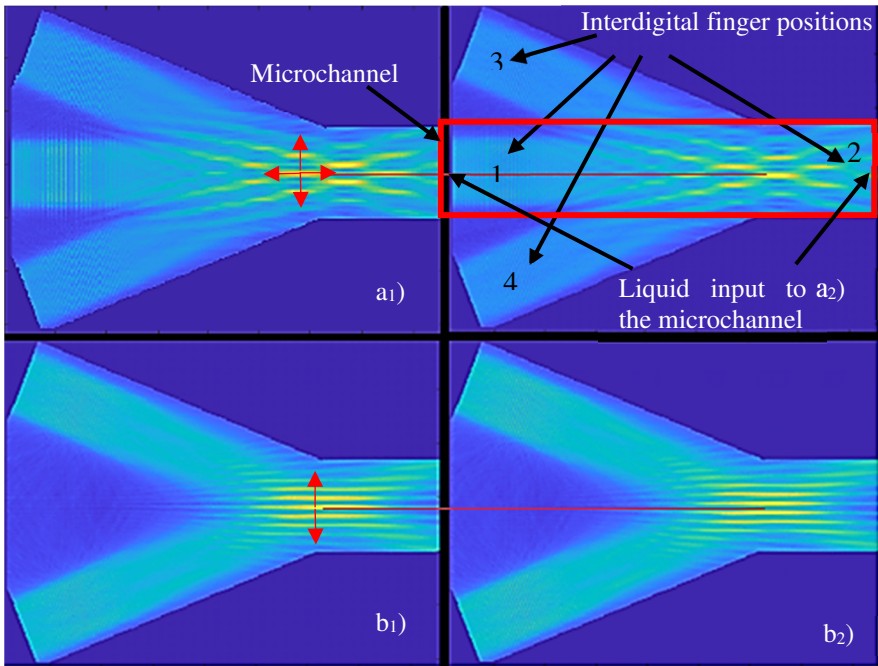


Fig. 19. Group interdigital finger interface in the x - y axis domain. Formation and control of pressure nodes (warmer colour)

In the presented model, the minimum and maximum pressure values are given in the x - z coordinate domain (see Fig. 18). Pressure effect simulation in the x - y coordinate domain of the microchannel was also performed using the FDTD method. Modelling methods were used to investigate the interaction of interdigital finger groups by monitoring the pressure structures induced by CMUT cells (see

Fig. 19). The model consists of 4 pairs of CMUT finger groups, which are marked as 1–4 in the figure. Each finger group consists of 20 pairs of fingers, when the spacing between fingers $\lambda = 300 \mu\text{m}$. Each group has integrated secondary fingers (together referred to as a pair of fingers), which are separated by the distance of $\lambda/4$ between the primary fingers. The parameters of the microchannel medium in the model are as follows: density is 997 kg/m^3 , and velocity of acoustic waves in water at 20°C is $1,481 \text{ m/s}$.

The solid-state foundation and microchannel parameters are eliminated by modelling the wave propagation effect in the liquid medium. Based on the design parameters of the CMUT cells, the transducers are excited by a constant 5 MHz sinusoidal signal. Since the model is made of two pairs of interdigital, the pairs of transducers are excited through a shift of -90° , which causes the ultrasonic energy to be directed to the center of the microchannel (1, 3, and 4 interdigital fingers), while the second interdigital finger pair is excited through a phase shift of $+90^\circ$. With respect to the horizontal axis, 3 and 4 finger groups are inclined at an angle of 22° .

The combined effect of interdigital fingers in the microchannel occurs when more than several finger groups are used. The FDTD modelling method simulates the effect of pressure fields when the liquid in the microchannel is exposed to several directional sources of acoustic waves. In the first case, the microchannel is modelled, which is marked as a red rectangle in the figure, and pressure structures (warmer colour) are visible. Scattered pressure structures are formed using 1, 3, and 4 finger groups (Fig. 19a). Due to the interdigital-induced pressure structure effect, this method is best suited for mixing and pumping liquids. Maintaining the excitement phase shift of interdigital pairs (-90° or $+90^\circ$) and changing the overall phase shift of interdigital groups in the model enables the positioning of the pressure structure in the microchannel in all directions of the x – y axis domain. By asserting the Gor'kov effect in the microchannel structure, the resulting pressure nodes are expected to accumulate materials smaller than λ .

In the second model (Fig. 19 b), only 3 and 4 finger groups were used. Changing the total finger group phase shift leads to a tunnel-type pressure structure formation. As it has been already mentioned, finger pairs have two pairs of fingers. The spacing between the fingers is $300 \mu\text{m}$, but the finger groups are turned at an angle of 22° relative to the horizontal axis. Due to these parameters, the pressure node will be longer than $300 \mu\text{m}$. Length can be calculated based on this formula:

$$\lambda_T = (1 - \sin(\sum_{i=0}^{\infty} \varphi_i)\lambda) + \lambda; \quad (3)$$

where λ_T – length of the pressure structure; φ_i – angle relative to the horizontal axis; λ – interdigital finger pair wavelength.

This method is proposed for use with an additional liquid pump. Adding active substance samples to the microchannel via the pump and changing the total third and fourth interdigital group phase shift allows this method to be used as a positioning system of biological elements on the analyte area in the microchannel.

CONCLUSIONS

1. It was determined that among the known signal processing methods applicable to the biosensor being created, the best signal to noise ratio is provided by a cross-correlation algorithm with an adaptive bandpass filter. This algorithm can achieve a signal to noise ratio of 65.56 dB in respect of a 30 ns informative delay signal.
2. The CNN algorithm of biosensor signal processing has shown that it can achieve a 15 dB better signal to noise ratio in comparison with other known signal processing methods.
3. A bovine serum albumin (BSA) deposition monitoring experiment on the microchannel analyte area showed that at different BSA concentrations the biosensor readings exhibited the typical BSA adsorption kinetics on the gold surface. We conclude that real-time biosensor data processing by the CNN algorithm may monitor the kinetics of biochemical interactions.
4. By varying the phase difference between the excitation signals of the interdigital-like structure, it is possible to achieve such a microstream arrangement that the liquid in the sensor microchannel is pushed, stirred or pumped.
5. The effective velocity of microparticle movement in the microchannel caused by acoustic microstreams was experimentally found to be 50 $\mu\text{m/s}$, when all CMUT structures in the sensor were excited harmonically and the phase difference between the excitation signals of the sensor structures was 90° . In this mode, the sensor transmits 4-pW net power to the microparticle stream while using about 16 mW of electrical power at the same time.
6. Simulations showed that the design of the biosensor is suitable for the precise positioning of biologically active microsized particles in the microchannel in both one-dimensional and two-dimensional coordinate systems. Such biosensor properties may be used for more sophisticated biochemical measurements because of their ability to manipulate different microparticles, separate them from each other, or merge microparticle streams.
7. Thermal loss measurements showed that the CMUT converter in the biosensor, excited harmonically, radiates an average of 14 mW of thermal power.

LIST OF REFERENCES

1. BHALLA, N., P. JOLLY, N. FORMISANO AND P. ESTRELA Introduction to biosensors. *Essays Biochem*, Jun 30 2016, 60(1), 1-8. Prieiga per doi: 10.1042/EBC20150001.
2. RODRIGUEZ-MOZAZ, S., M. P. MARCO, M. J. L. DE ALDA AND D. BARCELÓ Biosensors for environmental applications: Future development trends. *Pure and Applied Chemistry*, Apr 2004, 76(4), 723-752. Prieiga per doi: 10.1351/pac200476040723.
3. SAPELIAUSKAS, E., D. BARAUSKAS, G. VANAGAS AND D. VIRZONIS Surface micromachined CMUTs for liquid phase sensing. 2014 Ieee International Ultrasonics Symposium (Ius), 2014, 2580-2583. Prieiga per doi: 10.1109/ultsym.2014.0644.
4. EAIMKHONG, S. Label-Free Biodetection Using Capacitive Micromachined Ultrasonic Transducers (CMUTs) and Its Application for Cardiovascular Disease Diagnostics. *Journal of Nanomedicine & Nanotechnology*, 2012, 03(05). Prieiga per doi: 10.4172/2157-7439.1000144.
5. DEREK, C., V. LEROY, D. KAURIN, L. ARBOGAST, et al. Propagation of a transverse wave on a foam microchannel. *EPL (Europhysics Letters)*, 2015, 112(3), 34004. Prieiga per doi: 10.1209/0295-5075/112/34004.
6. ANDRIA, G., F. ATTIVISSIMO AND N. GIAQUINTO Digital signal processing techniques for accurate ultrasonic sensor measurement. *Measurement*, Sep 2001, 30(2), 105-114. Prieiga per doi: 10.1016/s0263-2241(00)00059-2.
7. HERGENRÖDER, R., J.-J. CHEN, F. WEICHERT, P. LIBUSCHEWSKI, et al. Real-time Low SNR Signal Processing for Nanoparticle Analysis with Deep Neural Networks 2018, 36-47. Prieiga per doi: 10.5220/0006596400360047.
8. FOGEL, R., J. LIMSON AND A. A. SESHIA Acoustic biosensors. *Essays Biochem*, Jun 30 2016, 60(1), 101-110. Prieiga per doi: 10.1042/EBC20150011.
9. RAMANAVICIENE, A., D. VIRZONIS, G. VANAGAS AND A. RAMANAVICIUS Capacitive micromachined ultrasound transducer (cMUT) for immunosensor design. *Analyst*, Jul 2010, 135(7), 1531-1534. Prieiga per doi: 10.1039/c0an00104j.
10. LECUN, Y., B. BOSER, J. S. DENKER, D. HENDERSON, et al. Backpropagation Applied to Handwritten Zip Code Recognition. *Neural Computation*, 1989, 1(4), 541-551. Prieiga per doi: 10.1162/neco.1989.1.4.541.

11. NEBAUER, C. Evaluation of convolutional neural networks for visual recognition. *IEEE Trans Neural Netw*, 1998, 9(4), 685-696. Prieiga per doi: 10.1109/72.701181.
12. SONKOLY, P., P. KOZMA, Z. NAGY AND P. SZOLGAY. Acoustic wave propagation modeling on 3D CNN-UM architecture. In *2006 10th International Workshop on Cellular Neural Networks and Their Applications*. 2006, p. 1-6.
13. GUIMING, D., W. XIA, W. GUANGYAN, Z. YAN, et al. Speech recognition based on convolutional neural networks 2016, 708-711. Prieiga per doi: 10.1109/siprocess.2016.7888355.
14. WIKLUND, M., R. GREEN AND M. OHLIN Acoustofluidics 14: Applications of acoustic streaming in microfluidic devices. *Lab Chip*, Jul 21 2012, 12(14), 2438-2451. Prieiga per doi: 10.1039/c2lc40203c.
15. MARSHALL, J. S. AND J. WU Acoustic streaming, fluid mixing, and particle transport by a Gaussian ultrasound beam in a cylindrical container. *Physics of Fluids*, 2015, 27(10), 103601. Prieiga per doi: 10.1063/1.4932232.
16. BRENNER, K., A. S. ERGUN, K. FIROUZI, M. F. RASMUSSEN, et al. Advances in Capacitive Micromachined Ultrasonic Transducers. *Micromachines (Basel)*, Feb 23 2019, 10(2). Prieiga per doi: 10.3390/mi10020152
17. LIU, K. K., R. G. WU, Y. J. CHUANG, H. S. KHOO, et al. Microfluidic systems for biosensing. *Sensors (Basel)*, 2010, 10(7), 6623-6661. Prieiga per doi: 10.3390/s100706623.
18. GUO, F., Z. MAO, Y. CHEN, Z. XIE, et al. Three-dimensional manipulation of single cells using surface acoustic waves. *Proc Natl Acad Sci U S A*, Feb 9 2016, 113(6), 1522-1527. Prieiga per doi: 10.1073/pnas.1524813113.
19. LU, Z. Estimating Time-of-Flight of Multi-superimposed Ultrasonic Echo Signal through Envelope 2014, 300-303. Prieiga per doi: 10.1109/cicn.2014.74.
20. ANDLE, J. C. AND J. F. VETELINO Acoustic wave biosensors. *Sensors and Actuators A: Physical*, 1994, 44(3), 167-176. Prieiga per doi: 10.1016/0924-4247(94)00801-9.
21. COLLINGS, A. F. AND F. CARUSO Biosensors: recent advances. *Reports on Progress in Physics*, 1997, 60(11), 1397-1445. Prieiga per doi: 10.1088/0034-4885/60/11/005.
22. MEHROTRA, P. Biosensors and their applications - A review. *J Oral Biol Craniofac Res*, May-Aug 2016, 6(2), 153-159. Prieiga per doi: 10.1016/j.jobcr.2015.12.002.
23. FU, Y. Q., J. K. LUO, N. T. NGUYEN, A. J. WALTON, et al. Advances in piezoelectric thin films for acoustic biosensors, acoustofluidics and

- lab-on-chip applications. *Progress in Materials Science*, 2017, 89, 31-91. Prieiga per doi: 10.1016/j.pmatsci.2017.04.006.
24. BAER, R. L., C. A. FLORY, M. TOM-MOY AND D. SOLOMON STW chemical sensors 1992, 293-298. Prieiga per doi: 10.1109/ultsym.1992.275993.
 25. THEVENOT, D. R., K. TÓTH, R. A. DURST AND G. S. WILSON *Electrochemical Biosensors: Recommended Definitions and Classification*. *Pure and Applied Chemistry*, 1999, 71(12), 2333-2348. Prieiga per doi: 10.1351/pac199971122333.
 26. *CRC Handbook of Chemistry and Physics*. 81st Edition Edited by David R. Lide (National Institute of Standards and Technology). CRC Press: Boca Raton, FL. 2000. 2556 pp. \$129.95. ISBN 0-8493-0481-4. *Journal of the American Chemical Society*, 2000, 122(50), 12614-12614. Prieiga per doi: 10.1021/ja0048230.
 27. LANGE, K., B. E. RAPP AND M. RAPP Surface acoustic wave biosensors: a review. *Anal Bioanal Chem*, Jul 2008, 391(5), 1509-1519. Prieiga per doi: 10.1007/s00216-008-1911-5.
 28. FERENTINOS, K. P., C. P. YIALOURIS, P. BLOUCHOS, G. MOSCHOPOULOU, et al. The Use of Artificial Neural Networks as a Component of a Cell-based Biosensor Device for the Detection of Pesticides. *Procedia Engineering*, 2012, 47, 989-992. Prieiga per doi: 10.1016/j.proeng.2012.09.313.
 29. IRANMANESH, I., M. OHLIN, H. RAMACHANDRAIAH, S. YE, et al. Acoustic micro-vortexing of fluids, particles and cells in disposable microfluidic chips. *Biomed Microdevices*, Aug 2016, 18(4), 71. Prieiga per doi: 10.1007/s10544-016-0097-4.
 30. LIU, Y. Z., B. J. KIM AND H. J. SUNG Two-fluid mixing in a microchannel. *International Journal of Heat and Fluid Flow*, 2004, 25(6), 986-995. Prieiga per doi: 10.1016/j.ijheatfluidflow.2004.03.006.
 31. RAHIMI, M., B. AGHEL, B. HATAMIFAR, M. AKBARI, et al. CFD modeling of mixing intensification assisted with ultrasound wave in a T-type microreactor. *Chemical Engineering and Processing: Process Intensification*, 2014, 86, 36-46. Prieiga per doi: 10.1016/j.cep.2014.10.006.
 32. VERHAAGEN, B., C. BOUTSIUKIS, L. W. VAN DER SLUIS AND M. VERSLUIS Acoustic streaming induced by an ultrasonically oscillating endodontic file. *J Acoust Soc Am*, Apr 2014, 135(4), 1717-1730. Prieiga per doi: 10.1121/1.4868397.
 33. LEE, H. J., K. K. PARK, P. CRISTMAN, O. ORALKAN, et al. The effect of parallelism of CMUT cells on phase noise for chem/bio sensor applications 2008, 1951-1954. Prieiga per doi: 10.1109/ultsym.2008.0481.

34. KHURI-YAKUB, B. T., K. K. PARK, H. J. LEE, G. G. YARALIOGLU, et al. 6D-1 The Capacitive Micromachined Ultrasonic Transducer (CMUT) as a Chem/Bio Sensor 2007, 472-475. Prieiga per doi: 10.1109/ultsym.2007.127.
35. MCLEAN, J. AND F. L. DEGERTEKIN Interdigital capacitive micromachined ultrasonic transducers for sensing and pumping in microfluidic applications 2003, 1, 915-918. Prieiga per doi: 10.1109/sensor.2003.1215624.
36. MCLEAN, J. AND F. L. DEGERTEKIN Directional scholte wave generation and detection using interdigital capacitive micromachined ultrasonic transducers. IEEE Transactions on Ultrasonics, Ferroelectrics and Frequency Control, 2004, 51(6), 756-764. Prieiga per doi: 10.1109/tuffc.2004.1304274.
37. SAPELIAUSKAS, E., G. VANAGAS, D. BARAUSKAS, M. MIKOLAJUNAS, et al. Design, simulation and testing of capacitive micromachined ultrasound transducer-based phospholipidic biosensor elements. Journal of Micromechanics and Microengineering, 2015, 25(7), 075013. Prieiga per doi: 10.1088/0960-1317/25/7/075013.
38. SAPELIAUSKAS, E., D. BARAUSKAS, G. VANAGAS AND D. VIRŽONIS Design, fabrication and testing of surface micromachined CMUTs for surface and interface waves. Elektronika ir Elektrotechnika, 2016, 22(5). Prieiga per doi: 10.5755/j01.eie.22.5.7123.
39. POTTY, G. R. AND J. H. MILLER Measurement and modeling of Scholte wave dispersion in coastal waters 2012, 500-507. Prieiga per doi: 10.1063/1.4765948.
40. DOMINGUEZ-MEDINA, S., S. MCDONOUGH, P. SWANGLAP, C. F. LANDES, et al. In situ measurement of bovine serum albumin interaction with gold nanospheres. Langmuir, Jun 19 2012, 28(24), 9131-9139. Prieiga per doi: 10.1021/la3005213.
41. LANGE, K., F. J. GRUHL AND M. RAPP Surface Acoustic Wave (SAW) biosensors: coupling of sensing layers and measurement. Methods Mol Biol, 2013, 949, 491-505. Prieiga per doi: 10.1007/978-1-62703-134-9_31.
42. GEDGE, M. AND M. HILL Acoustofluidics 17: theory and applications of surface acoustic wave devices for particle manipulation. Lab Chip, Sep 7 2012, 12(17), 2998-3007. Prieiga per doi: 10.1039/C2LC40565B.
43. SAPELIAUSKAS, E., D. BARAUSKAS, G. VANAGAS, D. PELENIS, et al. *Design, Fabrication and Testing of Surface Micromachined CMUTs for Surface and Interface Waves*. Edition ed., 2016. ISBN 2029-5731[escape].

44. QIN, J., C. STROUD AND F. DAI Noise Figure Measurement Using Mixed-Signal BIST 2007, 2180-2183. Prieiga per doi: 10.1109/iscas.2007.378606.
45. PELENIS, D., D. BARAUSKAS, E. SAPELIAUSKAS, G. VANAGAS, et al. Acoustical Streaming in Microfluidic CMUT Integrated Chip Controls the Biochemical Interaction Rate. *Journal of Microelectromechanical Systems*, 2017, 26(5), 1012-1017. Prieiga per doi: 10.1109/jmems.2017.2701144.
46. PELENIS, D., D. BARAUSKAS, G. VANAGAS, M. DZIKARAS, et al. CMUT-based biosensor with convolutional neural network signal processing. *Ultrasonics*, Jul 2 2019, 99, 105956. Prieiga per doi: 10.1016/j.ultras.2019.105956.
47. ROCHA-GASO, M. I., C. MARCH-IBORRA, A. MONTOYA-BAIDES AND A. ARNAU-VIVES Surface generated acoustic wave biosensors for the detection of pathogens: a review. *Sensors (Basel)*, 2009, 9(7), 5740-5769. Prieiga per doi: 10.3390/s90705740.

LIST OF PUBLICATIONS ON THE TOPIC OF THE THESIS

Publications in the Institute for Scientific Information Web of Science database with the citation index

1. Pelenis, Donatas; Barauskas, Dovydas; Vanagas, Gailius; Dzikaras, Mindaugas; Viržonis, Darius. CMUT-based biosensor with convolutional neural network signal processing // *Ultrasonics*. Amsterdam: Elsevier B.V. ISSN 0041-624X. eISSN 1874-9968. 2019, vol. 99, art. no. 105956, p. 101-110. DOI: 10.1016/j.ultras.2019.105956.
2. Pelenis, Donatas; Dzedzickis, Andrius; Morkvėnaitė-Vilkončienė, Inga; Bučinskas, Vytautas; Barauskas, Dovydas; Vanagas, Gailius; Mikolajūnas, Marius; Katkus, Justinas; Viržonis, Darius. Non-contact sensing of elastic modulus of the UV cured furniture coatings by the transverse acoustical waves // *IEEE sensors journal*. Piscataway, NJ: IEEE. ISSN 1530-437X. eISSN 1558-1748. 2018, vol. 18, iss. 16, p. 6527-6532. DOI: 10.1109/JSEN.2018.2850362.
3. [S1; US] Pelenis, Donatas; Barauskas, Dovydas; Sapeliauskas, Evaldas; Vanagas, Gailius; Mikolajūnas, Marius; Viržonis, Darius. Acoustical streaming in microfluidic CMUT integrated chip controls the biochemical interaction rate // *Journal of Microelectromechanical Systems*. Piscataway, NJ : IEEE. ISSN 1057-7157. eISSN 1941-0158. 2017, Vol. 26, iss. 5, p. 1012-1017. DOI: 10.1109/JMEMS.2017.2701144.
4. [S1; LT] Sapeliauskas, Evaldas; Barauskas, Dovydas; Vanagas, Gailius; Pelenis, Donatas; Viržonis, Darius. Design, fabrication and testing of surface micromachined CMUTs for surface and interface waves // *Elektronika ir elektrotechnika*. Kaunas: KTU. ISSN 1392-1215. eISSN 2029-5731. 2016, vol. 22, iss. 5, p. 69-73. DOI: 10.5755/j01.eie.22.5.7123.

5. [S1; US] Barauskas, Dovydas; Pelenis, Donatas; Viržonis, Darius; Baltrus, John P.; Baltrušaitis, Jonas. Greenhouse gas molecule CO₂ detection using a capacitive micromachined ultrasound transducer // Analytical Chemistry. Washington, NW : ACS Publications. ISSN 0003-2700. eISSN 1520-6882. 2016, Vol. 88, iss. 13, p. 6662-6665. DOI: 10.1021/acs.analchem.6b02085.

INFORMATION ABOUT THE AUTHOR OF THE THESIS

Date and place of birth: July 6, 1991, Panevėžys.

Education: 1998 – 2010 – Smilgiai secondary school;
2010 – 2013 – bachelor's degree in Electrical and automation equipment at Panevėžys University of Applied Sciences;
2013 – 2015 – master's degree in Control Technologies at Kaunas university of Technology;
Contacts: donatas@pelenis.lt, tel.: +370 655 33156.

REZIUMĖ

Darbo aktualumas

Šiais laikais biojutikliai yra plačiai taikomi įvairiuose mokslo srityse. Medicinoje jie yra naudojami navikų, patogenų, padidėjusiam gliukozės kiekiui kraujyje aptikti ir toksinų detekcijai. Jau kelis dešimtmečius mokslininkai, tyrėjai dirba, vystydami įvairių biojutiklių technologijas [2, 8], kurios leidžia diagnozuoti, įvertinti ir stebėti su biologiniais elementais vykstančius procesus, užtikrinant kokybinius ir kiekybinius parametrus. Šiuo metu biojutiklinės sistemos klasifikuojamos pagal taikymo būdą ir detekcijos sritis. Priklausomai nuo taikomo transdukcijos principo, jie skirstomi į: elektrocheminius, masės ir optinius [24-27]. Taip pat biojutiklinės sistemos gali veikti kaip klasifikatoriai, kurie geba įvertinti baltymų, nuklerino rūgščių, enzymų, sacharidų oligonukleotidų ir ligandų sąveikos procese vykstančius pokyčius. Remiantis aptiktos analitės tipais, biojutiklinės sistemos gali būti modifikuojamos DNR, gliukozės, toksinų, mikrotoksinų, vaistų ar fermentų detekcijai. Dažniausiai biodetektuojant, stebima sąveikos su biologiniais elementais kiekybiniai parametrai, pavyzdžiui antikūno susijungimas su antigenu [6, 28, 29].

Ankstesni moksliniai tyrimai parodė, kad biologinių elementų detekcijai gali būti taikomi ir talpiniai mikromontuojami ultragarsiniai keitikliai (CMUT), kurių gaminimo, veikimo ir taikymo būdai skiriasi nuo pjezoelektrines medžiagas naudojančių MEMS biojutiklių. Kiekviena vystoma biojutiklinė technologija reikalauja spręsti tiek su technologiniais kūrimo ir aptarnavimo procesais, tiek su biocheminės sąveikos analizės metodais susijusias problemas. Ne išimtis ir CMUT pagrindu veikiančios biojutikliai. Darbe naudojamas skysčio ir kieto kūno sandūroje sklindančios skersinės akustinės bangos biojutiklis, kuris pritaikytas dirbti skysčių terpėje ir gali veikti tiek kaip biologinės sąveikos aptikimo, stebėsenos jutiklis, tiek kaip mikrosrautų valdymo, biologiškai aktyvių elementų

pozicionavimo įtaisais. Anksčiau sukurtos biojutiklių versijos [2] turi eilę techninių trūkumų, susijusių su įvairaus pobūdžio instrumentiniu ir natūraliu triukšmu. Prie natūralaus triukšmo šaltinių priskirtini biologinės kilmės medžiagoms specifiniai efektai: baltymų degeneracija, denatūracija ir kitokie biocheminiai efektai, kurie nuolat vyksta bioaktyviose sistemose. Šie efektai negali būti stabilizuoti techninėmis priemonėmis, todėl reikalingas specifiniai signalo apdorojimo būdai, turintys didelį atsparumą neinformatyviems trikdžiams. Sužadinta akustinė banga biojutiklyje sklinda visais jutiklio konstrukcijos elementais: silicio pagrindu, skysčiu, mikrokanalo sienelėmis. Tuo tarpu, naudingą informaciją neša skersinės Šoltė tipo bangos sklidimo laikas ir energetiniai jos pokyčiai, todėl biojutikliuose būtinas signalo apdorojimo algoritmų lankstumas ir pritaikomumas eliminuojant neinformatyviuosius trikdžius. Tokiomis sąlygomis įvertinant jutiklio rodmenis geriausiai veikia daugiaparametriniai algoritmai, kuriais remiantis gali būti išmatuojami biologinės sąveikos sukelti informatyvios bangos pokyčiai. Dėl energijos konversijos efektyvumo CMUT technologija yra tinkama taikyti ne tik kaip aplinkos ar sąveikos įvertinimo įtaisais, bet ir kaip vykdymo įtaisais, skirtas tiksliai bioaktyvių elementų pozicionavimui mikrokanale. [17, 30-32].

Darbo tikslas – sukurti CMUT šukų tipo struktūrą turinčių biojutiklių skersinės bangos vėlinimo matavimo metodą ir būdą, turintį padidintą atsparumą įvairių triukšmo šaltinių atžvilgiu.

Mokslinė problema

Ankstesni tyrimai parodė, kad mechaninis, dinaminis biologinių elementų savybių matavimas MEMS įtaisais yra parankus kiekybinei ir kokybinei bioelementų diagnostikai. Iš kitos pusės, koks bebūtų didelis rezonansinio CMUT keitiklių veikimo jautrio potencialas, rezonansinis režimas nėra tinkamas realiuoju laiku veikiantiems biojutikliams dėl didelio slopinimo veikiant skystyje. Kadangi CMUT tipo biojutiklį sudaro dvi CMUT siūstovo ir imtuvo šukų tipo struktūros bei biojutiklio viduryje analitei skirta aikštelė, biocheminė sąveika gali būti aptinkama matuojant akustinių bangų vėlinimą. Vis dėl to, žinomi signalo apdorojimo metodai ne visada tinka apdoroti tokia CMUT struktūra gautiems signalams. Informacija gaunama iš daugiau nei vieno tuo pačiu metu veikiančio kanalo, o santykis signalas-triukšmas yra mažas. Dėl signale esančio triukšmo ir atsako signalo kompleksiško susiduriama su signalo apdorojimo greitaveikos ir jutiklio jautrio apribojimais. Todėl reikalinga santykį signalas-triukšmas gerinanti jutiklio signalų apdorojimo ir interpretavimo metodika, kuri būtų tinkama ekonomiškai pagrįstai techninei realizacijai. Taip suformuluota problema šiame darbe sprendžiama kuriant ir tiriant inovatyvų signalų apdorojimo metodą, pagrįstą konvoliucinio dirbtinio neuroninio tinklo, galinčio veikti su mikrovaldikliais, mikrokompiuteriais ar programuojamomis loginėmis matricomis, panaudojimu.

Darbinė hipotezė

Taikant specifinius, dideliu lankstumu ir adaptyvumu pasižyminčius signalų apdorojimo algoritmus, galima reikšmingai pagerinti Scholte tipo bangų vėlinimo matavimo principu veikiančių biojutiklių naudingo signalo ir triukšmo santykį. Biojutiklio elektromechanines struktūras, normaliai naudojamas bangos vėlinimo matavimui, galima panaudoti analitinių skysčių pumpavimui, maišymui ir biologiškai aktyvių dalelių pozicionavimui vienos ar dviejų ašių sistemoje, pakaitomis su jutiklio funkcija.

Darbo uždaviniai

1. Ištirti žinomus skersinės akustinės bangos vėlinimo matavimo metodus bei galimybes juos pritaikyti CMUT pagrindu veikiančiam biojutikliui.
2. Sukurti ir ištirti dirbtinio neuroninio tinklo pagrindu veikiančių akustinės bangos vėlinimo matavimo algoritmą, pritaikytą CMUT biojutikliui ir kiekybiškai palyginti jį su žinomais algoritmais ir matavimo būdais.
3. Naudojant naujai sukurtą algoritmą atlikti biologiškai aktyvių elementų nusodinimo biojutiklio analitinėje zonoje stebėsenos eksperimentus ir juos charakterizuoti.
4. Ištirti galimybes biojutiklio CMUT elektromechaninę struktūrą panaudoti mikrosrautų pumpavimui, maišymui bei biologiškai aktyvių dalelių pozicionavimui.
5. Charakterizuoti mikrosrautų pumpavimą energetiniu požiūriu.
6. Ištirti galimybes CMUT jutiklio mikrostruktūromis pozicionuoti biologiškai aktyvias daleles vienos ir dviejų ašių koordinacinių sistemose.
7. Įvertinti biojutiklio, veikiančio harmoniniu režimu, šiluminius nuostolius.

Mokslinė vertė

1. Sukurti biojutiklio signalo apdorojimo metodai ir skaitmeniniai bei analitiniai modeliai leis tiksliau interpretuoti vykstančias biochemines sąveikas CMUT biojutiklio mikrokanale, lanksčiai adaptuojantis prie kintančių matavimo terpės ir mikrokanalo parametrų.
2. Darbe pademonstruotas dirbtiniu neuroninio tinklo pagrindu veikiančio signalo apdorojimo algoritmas leis sukurti signalo apdorojimo sistemą, pasižyminčią išskirtiniu atsparumu triukšmui ir matavimo sąlygų slinkčiais.
3. Sukurtas akustinio srauto mikrokanale modeliavimo metodas, leidžiantis modeliuoti fazuotomis CMUT pirštų grupėmis sužadintas akustines bangas. Šiuo metodu grindžiama biologinių elementų, skysčio manipuliacijos ir nusodinimo metodika CMUT biojutiklio mikrokanale.

Darbo rezultatų praktinė vertė

Darbo metu gautos žinios leis supaprastinti CMUT tipo biojutiklių, dirbančių mikroskysčių aplinkoje, kalibravimą ir gauti geresnį santykį

signalas/triukšmas, sumažinant priklausomybę nuo matavimo terpės ir kitų matavimo sąlygų įtakos. Sukurti signalo apdorojimo ir akustinių bangų modeliavimo metodai bus panaudoti projektuojant prototipinių biojutiklių struktūras ir jų veikimą užtikrinančią elektroniką.

Ginamieji teiginiai

1. Pritaikant dirbtinius neuroninius tinklus CMUT biojutiklio signalo apdorojimui, galimas iki 15 dB santykio signalas/triukšmas pagerėjimas;
2. Biocheminės sąveika gali būti aptikta interpretuojant skersinių bangų, sklindančių tarp skysto ir kieto kūno, vėlinimo kinetiką;
3. Šukų tipo CMUT struktūrą turintis biojutiklis gali būti panaudojamas ir kaip vykdymo įtaisas, valdantis biologiškai aktyvių dalelių padėčių vienos ar dviejų ašių sistemoje.

Darbo aprobavimas

Pagrindiniai daktaro disertacijos tyrimų rezultatai aprobuoti 5 publikacijose mokslinės informacijos instituto (ISI) pagrindinio sąrašo leidiniuose su citavimo indeksu ir 2 pranešimais tarptautinėse mokslo konferencijose.

Disertacijos struktūra ir apimtis

Disertaciją sudaro įvadas, 4 skyriai, išvados, naudotos literatūros sąrašas ir autoriaus publikacijų sąrašas. Bendra disertacijos apimtis yra 99 puslapis, 44 paveikslai, 3 lentelės, 125 bibliografinės nuorodos.

IŠVADOS

1. Nustatyta, kad iš žinomų kuriamam biojutikliui pritaikomų signalo apdorojimo metodų geriausią santykį signalas - triukšmas užtikrina kryžminės koreliacijos algoritmas su adaptyviu juostiniu filtru. Šiuo algoritmu 30 ns naudingo vėlinimo signalo atžvilgiu galima pasiekti 65,56 dB santykį signalas - triukšmas.
2. Ištyrus biojutiklio signalo apdorojimą CNN algoritmu nustatyta, kad juo galima pasiekti 15 dB geresnį santykį signalas - triukšmas, nei taikant žinomus signalo apdorojimo metodus.
3. Iš galvijų serumo albumino (GSA) nusodinimo mikrokanalo analitinėje zonoje stebėsenos eksperimento nustatyta, kad biojutiklio rodmenys įvairių GSA tirpalo koncentracijų atvejais pasižymi GSA adsorbicijai aukso paviršiuje būdinga kinetika. Darome išvadą, kad realiuoju laiku renkamus biojutiklio duomenis apdorojant CNN algoritmu, galima stebėti biocheminės sąveikos kinetiką.
4. Įvairiai keičiant fazių skirtumą tarp šukų tipo struktūros žadinimo signalų galima pasiekti tokio mikrosrautų išsidėstymo, kad jutiklio mikrokanale esantis skystis būtų stumiamas, maišomas ar pumpuojamas.
5. Eksperimentiškai ištirtas efektyvus akustinių mikrosrautų sukeltas mikrodalelių judėjimo greitis mikrokanale siekė 50 $\mu\text{m/s}$., kai visos jutiklyje esančios CMUT struktūros žadinamos harmoniniu būdu, o fazių skirtumas

tarp jutiklio struktūrų žadinimo signalų yra 90° . Tokiu režimu veikiantis jutiklis mikrodalelių srautui perduoda 4 pW naudingos galios, tuo pačiu metu naudodamas apie 16 mW elektrinės galios.

6. Modeliuojant parodyta, kad biojutiklio konstrukcija yra iš esmės tinkama tiksliam biologiškai aktyvių mikroninių matmenų dalelių pozicionavimui mikrokanale tiek vienmatėje, tiek dvimatėje koordinačių sistemoje. Tokios biojutiklio savybės gali būti panaudotos žymiai sudėtingesniems biocheminiams matavimams, nes suteikia galimybę manipuluoti skirtingomis mikrodalelėmis, jas atskirti vienas nuo kitų arba sulieti mikrodalelių srautus.
7. Šiluminių nuostolių matavimai parodė, kad žadinamas harmoniniu būdu biojutiklyje esantis CMUT keitiklis vidutiniškai spinduliuoja 14 mW šiluminę galią.

UDK 681.586.48+53.082.9](043.3)

SL344. 2020-*,* leidyb. apsk. I. Tiražas 50 egz.

Išleido Kauno technologijos universitetas, K. Donelaičio g. 73, 44249 Kaunas
Spausdino leidyklos „Technologija“ spaustuvė, Studentų g. 54, 51424 Kaunas